APPLICATIONS OF RESISTIVITY METHODS AND MICRO-EARTHQUAKE MONITORING IN GEOTHERMAL EXPLORATION

MULYADI*
UNU Geothermal Training Programme
National Energy Authority
Grensásvegur 9,
108 Reykjavik
ICELAND

*Permanent address:
PERTAMINA
GEOTHERMAL DIVISION
Jalan : Kramat Raya 59,
Jakarta Pusat,
Jakarta,
INDONESIA.

ABSTRACT

This report contains two chapters, describing resistivity methods and micro-earthquake monitoring applied to explore geothermal resources.

Four resistivity methods with their applications in geothermal areas, i.e. Schlumberger, Head-on, and Wenner, Dipole-dipole used for exploration at Broadlands (New Zealand) and Hvitholar (Iceland), respectively, are observed. The combinations of resistivity data of Schlumberger and Head-on may probably be useful to construct 2-D resistivity model.

The hypocenters of micro-earthquakes monitored in the period of six months at Lahendong, Indonesia, were originally calculated by using single layer velocity model. While in this study, they were recalculated by using multiple layer velocity model. The events significantly cluster outside the caldera rim and only a few are located inside the caldera at relatively shallow depth. This phenomenon may be due to fracturing along the contact area between hot fluids and cool rocks, or, hot rocks and meteoric water at depth. The distribution of hypocenters could also be the result of the combination of overburden pressure and temperature. Hence, the number of events reaches a maximum at depths of about 2-3 km reflecting either the depths of the highest rate of volumetric contraction or high heat flow in the area.

TABLE OF CONTENTS

List of Tables

List of Figures

INTRODUCTION

This report is intended to complete the six months United Nations University (UNU) Geothermal Training Programme held at the National Energy Authority (N.E.A), Iceland. It contains two chapters, describing resistivity methods applied to explore geothermal resources with case histories at Broadlands, New Zealand, and Hvitholar, Iceland, and micro-earthquake monitoring at Lahendong geothermal area, Indonesia.

Of the geophysical techniques, electrical methods are most useful and commonly employed in geothermal exploration, with some being used for monitoring too. Each method has its advantages and disadvantages, depending on the setting, purposes and targets of investigations.

In the micro-earthquake monitoring method, relocating the events have been done to observe if there are any discrepancies between original and relocated events. Studies of hypocenters distribution in relating to the geothermal system are presented.

PART ONE

1. REVIEW OF RESISTIVITY METHODS

The various resistivity methods have different capabilities in probing depth, and in detecting lateral and vertical resistivity changes. Problems arise when combinations of methods yield different results. Basically the parameters that characterize a geothermal system, e.g. high temperature, alteration mineral like clays, the presence of electrolyte aqueous solution, etc, may cause low resistivity anomalies.

The purpose of these methods is to probe the resistivity changes with depth as well as map-out lateral contrasts. Changing current flows through a formation in the earth results in changing the potential difference at a field rectangular to the current field. This current field is artificially induced by injecting the current into the earth. However, natural current flow can be created occasionally due to (1) the interaction of solar wind with the earth's magnetic field and ionosphere below 1 Hz, (2) worldwide thunderstorms above 1 Hz, and (3) electrochemical, electrokinetic and thermoelectric sources within the earth. The probing depths of injected current is related to the electrode array. Different arrays are used for geothermal exploration depending on to the depths of investigations.

1.1. Basic Theory of Resistivity

In this report there is no attempt to discuss in detail the theory behind resistivity, and only the basic mathematical is presented. The following equation show the potential difference, V, at a point due to a point source located at distance, r(m), emanating a current, I(mA), in a homogeneous medium with resistivity, $\Gamma(\Omega m)$, :

$$V = (I*\Gamma)/(2*\pi*r)$$

For practical work, the current is injected through two current electrodes which behave as source and sink. Then the potential difference of V at a point with a distance of r_1 from the source and r_2 from the sink is :

$$V = (I*\Gamma)/(2*\pi) * (1/r_1 - 1/r_2)$$

By measuring the potential difference, V(mV), due to injected current, I(mA), one can calculate the apparent resistivity :

$$\Gamma_{app.} = (V/I)/G \qquad (1)$$

where $\Gamma_{app.}$ and G are apparent resistivity (in Ωm) and geometric factor which varies with the electrode arrays, respectively.

1.2. Solving Rising Problems

1.2.1. Topography

The effect of topography can be solved by avoiding rough terrain in the field and by 2-D modelling which is done in the office.

1.2.2. Inhomogeneity

Surface inhomogeneity such as thermal manifestations and the water-logged grounds of a tropical bush may distort the observed apparent resistivity. For example, setting the potential electrodes on inhomogeneous media would result too higher current density in the conductive media rather than in the resistive one, thus affecting potential drop inversely. For inhomogeneities with dimensions much smaller than current electrodes spacing and located very close to the current electrodes are considerably less harmful; the electrical current field may resume its normal pattern away from them. One should have at least a qualitative understanding of the effects of inhomogeneities parallel to the traverse line.

In some methods, such as Schlumberger, problem may arise even if the potential electrodes are set on homogeneous media. Nevertheless, a sounding resistivity curve distorted by surface inhomogeneity may not be resolved during curve interpretation. The problems might be overcome by taking into account the various potential differences in accordance with the neighboring current point sources, hence applied a 2-D resistivity computer program.

1.2.3. Practical field operation and portability of instruments

A compass and tape measure are used to define the traverse lines. An error of AB spacing due to a bend of traverse line is very small, about 3% error for an angle of about 10°. Field measurements can be made convenient and less time-consuming by employing portable instruments especially in heavy terrain areas. The receiver itself is usually very light.

1.2.4. Data processing

The observed resistivity data are usually presented as a 1-D model as apparent or true resistivity profiles, apparent and true resistivity maps at certain AB/2 and depths, respectively. While a 2-D model is commonly presented as the true resistivity layering.

Inverting the observed apparent resistivity data into resistivity layers can be done by either using classical curve matching or numerical solution methods. The former is usually used to get a preliminary interpretation with no sophisticated computer involved. While the latter is done for detailed interpretation. It was shown that the apparent resistivities in both Schlumberger and Wenner arrays at the small and large electrode spacings tend to be the true resistivity of the first and last layers, respectively. Projecting a sounding curve into layer resistivities may be not so difficult since the curve is Hummel type.

The layer thickness can be directly estimated from the axis (AB/2,m) by assuming that the dept of the layers is equal to the sum of the layers with the resistivity values read at the y-axis. But for the other types of the sounding curves, e.g. A, Q and K, the depths of layers are less than the sum of the layers. Many methods have been modified to get sophisticated results, and these usually involve the conversion of the sounding data to Kernel function using Ghosh filter and determined layering parameters from the Kernel function using, for example, Koefoed (1979) methods. The 1-D inversion computer program, (N.E.A., Iceland), which is called Ellipse, was used in this report to inverse the sounding data measured in 1983 at the Hvitholar geothermal area. This resistivity program mainly applies a linear filter and automatic iteration methods. Moreover, the program considers the standard deviation and number of readings of potential differences to determine the averages of potential values. A problem may arise when the contrast resistivity between successive layers become too large, thus giving a sharp slope of the sounding curve. Whereas the maximum theoretical slope is 45°. A quantitative understanding of the correlations of the resistivity layer with the surrounding zone is desirable.

The 2-D resistivity computer program applying finite element method, (Sigurdsson, 1986), was also used in this report to model the E-W resistivity structure at the Hvitholar area. The program calculates the apparent resistivity of Schlumberger, Dipole-dipole and Head-on arrays at depths for given arbitrary grid spacing of layer resistivities model.

1.3. Resistivity Array Method

1.3.1. Schlumberger and Head-On

1.3.1.1. Schlumberger

Early attempts to measure resistivities in geophysical exploration were based on the two electrode approach rather than on the four electrode approach. The Schlumberger method is described first because it is one of the most common method used to investigate geothermal prospects nowadays, and has been applied since 1920, after the works of Wenner in 1915. The topography effect is stronger at short AB spacing and shallow depth since the current will flow parallel to the terrain, rather than at deeper levels and larger spacings. Hence, this method has great advantage in investigating a deep target rather then shallow formations. Geothermal reservoirs, for example, may lie in the range of 500 m to 2500 m depth, thus requiring only 1000 to 5000 m length of cable since the probing depth is equal to or less than AB/2. To overcome topographic effects the 2-D computer program may be used to calculate the potential at the undulation surface. The Schlumberger method may give a false picture of the lateral and vertical resistivity distributions. Within an area where surface conductivity spreads over several zones and a thick conductive overburden which absorbs current thus the layer underneath the conductive layer is unprobed.

The geometric factor can be calculated from the symmetrical electrode array as :

$$G = 2*\pi \,/(\, 1/AM - 1/AN + 1/BN - 1/BM \,)$$

where :
AB and MN are current and potential electrodes armlengths in meters, respectively.

The apparent resistivity ($\Gamma_{app.}$) can then be calculated using equation (1) by injecting a current through current electrodes AB and then measuring the potential difference at MN.

1.3.1.2. Head-On

This method is an improvement of the half Schlumberger array and it is very simple interpreting the observed data into resistivity structures.

However, the method needs a long cable with a length of about to be equal to or higher than eight times the AB-current electrode spacing used to create the infinite current source, see Figure 2. It was previously applied in China, which has then been introduced in New Zealand, (Cheng, 1980). It has been successfully applied in geothermal areas in Iceland to detect fracture zones which create a high resistivity contrast, e.g. the Krafla-Hvitholar geothermal field, (Arnason et al., 1984).

The geometric factor is simplified to the following relationships due to AC, BC, CM, and CN are infinite :

$$G = 2*\pi/(1/AM-1/AN),$$

and

$$G = 2*\pi/(1/BM-1/BN),$$

for current electrodes AC and BC, respectively.

1.3.2. Wenner And Dipole-Dipole

1.3.2.1. Wenner

The electrode array consists simply of four equally spaced and collinear electrodes, see Figure 3. The probing depth is about the same as that of AM spacing. The method is most effective in flat or gentle terrain but poses problems in geothermal areas in andesitic volcanic settings where the topography is rough. One needs a wide flat area to probe deeper resistivity

changes that is often absent in such settings, for example, to probe at depth of about 500 m, a 1500 m (3*a) long wire must be laid out.
Collecting and processing the resistivity data are very similar to the method of Schlumberger array.

The apparent resistivity, ($\Gamma_{app.}$), can be calculated from the following equation :

$$\Gamma_{app.} = 2*\pi*a*(V/I)$$

1.3.2.2. Dipole-Dipole

Some of the limitations of both the Wenner and Schlumberger arrays can be overcome by using the Dipole-dipole method. Al'pin (1950), had suggested a modification of the use of the standard resistivity method which could probe deeper without using longer cables, e.g. Dipole-dipole. The basic advantages are as follows: a) simultaneous measurement of vertical and lateral resistivity variations, b) reduce leakage errors at both the current and potential cables which is commonly present in the practice, c) adaptability to rough terrain, in as much as cables required are not too long. However, inverting observed resistivity data into the 1-D layer resistivities is practically very difficult. The various electrode configurations is shown in Figure 4.

The Dipole-dipole method is mainly used to detect lateral changes in resistivity that may be due to faults, fractures, and litho-logical contacts, rather than vertical changes in resistivity as in the Schlumberger method.

The coincidence between theoretical curves for Schlumberger and Equatorial dipole arrays holds only for a medium in which the resistivity does not vary laterally, (Keller, 1966). Despite this fact, Koefoed (1979), described the conversion of apparent resistivity Dipole-dipole into apparent resistivity Schlumberger method by using the Patella method.

2. WENNER AND DIPOLE-DIPOLE METHODS APPLIED AT BROADLANDS GEOTHERMAL FIELD, NEW ZEALAND

The resistivity methods of Wenner and dipole-dipole had been successfully applied in the Broadlands geothermal fields, New Zealand. The lateral extent of the Broadlands reservoir was first determined by the Wenner method with electrodes spacing of a = 180, 550, and 1100 m, (Risk et al., 1970). The area can be seen in Figure 5, with the locations of wells, temperatures at 500 m depth and rate of steam flow. Good geothermal production zones must have high temperatures as well as high permeability. However, permeable zones cannot be predicted from these measurements. For example, a high resistivity anomaly was mapped out (at north west corner in Figure 5) where wells later produced high steam flow where as there was negligible steam flow within low resistivity anomaly. It is noteworthy that the apparent low resistivity delimited the extent of the hot water reservoir; however the results can not be used merely for locating drillholes to find the reservoir. Besides the Wenner array, Dipole-dipole was also applied in Broadlands. The method is similar to the maximum array discussed by Keller (1966), modified a little bit by Risk et al. (1970). The current source was injected through any two of three current electrodes (A,B,C) and the potential drop was measured through a pair of potential electrodes which were place at rectangular positions. The geothermal field boundary defined using this method is similar to that of the Wenner method, see Figure 5.

3. SCHLUMBERGER AND HEAD-ON METHODS APPLIED AT HVITHOLAR GEOTHERMAL AREA

3.1. Geological setting

The Hvitholar geothermal area is part of the Krafla geothermal field, which lies within the south edge of the Krafla caldera, in the Neovolcanic zone (north eastern Iceland), characterized by two active fracture trends i.e. a N-S fissure swarm and E-W fracture trends. Such structures may indicate the possibility of a geothermal reservoir. Until 1979 when steaming ground was observed, there had been no reported active geothermal manifestation in the area.

3.2. Review of the Geothermal Area

A shallow large magma chamber detected by seismic studies over the area, most likely causing the high subsurface temperatures. Geochemical surveys indicated the presence of three major upflow zones, i.e. Leirhnjukur, Hveragil and the area south of Mt. Krafla, (Armansson et al.,1982), however no description are available yet for the Hvitholar area.

About 23 wells have been drilled in the low resistivity anomaly, i.e. wells KJ (1-13, 15), (14, 16-20), and (21-23) at Leirbotnar, the southern slope of Mt. Krafla and Hvitholar area respectively, (Sigurdsson et al., 1985).

The higher reservoir pressure in the well KJ-21 compare to the wells KJ-22 and KJ-23 indicates a westward flow direction, (Wale, 1985). KJ-23 is, in fact, an unproductive well, even though the reservoir temperature was high enough (about 250°C).

About 30 resistivity soundings (Schlumberger) were measured and also at the same time four lines of resistivity Head-on were measured in the N-S and E-W directions over the Hvitholar geothermal area, (Arnason et al., 1984).

The resistivity substructure had been previously modelled by calculating apparent resistivity sounding independently from the apparent resistivity of Head-on, because the unavailability, then, of a computer program to calculate the apparent resistivities of different methods simultaneously, see Figure 6. In this study, the calculated apparent resistivities of both Schlumberger and Head-on methods will be presented.

3.3. Resistivity Modelling

Eight measured resistivity sounding data were inverted into 1-D layer resistivity model with the Ellipse program, utilizing the Vax computer installed at the National Energy Authority, Iceland. These results were then used to construct a 2-D resistivity model by simply joining resistivity layers. Afterwards the Head-on apparent resistivities were taken into consideration. The 2-D resistivity model is modified until there is good match between the calculated and observed apparent resistivities both for Sounding and Head-on by the trial and error method, see Figure 7. The apparent resistivity soundings calculated at places from the west to the east, Kr115 , 114, 109, 108, 106, 105, 116, and 122, appear practically similar to that of the observed ones, especially at deep levels, as can be seen in Figures 8a and b. The calculated apparent resistivities of Head-on method gave a good match, for AB/2 = 250, 500, and 750 m, see Figure 9a, b, and c. The poor match at the west end of the section for AB/2 = 250 m, is due to the topographic effects where the measurements had been carried out in the valley, (Eyjolfsson, pers. comm.).

To get an impression of the locations of wells in relation to geothermal system in this area, the top conductive (is less than 20 Ωm) layers and the resistivity variations within the conductive layers are plotted, see Figure 10 and 11. The top conductive layers in perspective viewing at angle of tilt and rotation of 30° and 225°N, respectively, were plotted (see Figure 12) although the locations of wells were just approximated due to the limited capability of the program. It still shows

a fault-like structure with a N-S strike at the top conductive layers but it is not clear at the bottom; the structure may be hidden.

4. DISCUSSION

The Wenner and Dipole-dipole methods were successfully used in delineating the reservoir boundary in New Zealand, due perhaps to the relatively flat topography and the lack of abrupt variations in resistivity. However, the effectiveness of the Wenner array is not yet fully assessed since the subsurface resistivity structures have not been modelled yet, and the apparent resistivity values have not been compared to observed ones.

It is unlikely that changing the 2-D resistivity model in order to fit the calculated and observed apparent resistivities at Kr108 could be resolved by maintaining the Head-on data unchanged. Discrepancies in the resistivity sounding curve may be caused by the presence of a low resistivity zone of altered rocks underneath Kr114, since the soundings situated far away were not affected. However, the conductive layers do not affect the nearby sounding Kr115, since it is located at the edge of the fine grid model where the resistivity structure of the adjoining area is not taken into account. In the Schlumberger method, it is assumed that the layer resistivities will be laterally homogeneous but not vertically. Hence, this method works very well in observing variations of resistivity changes with depth. In contrast, the Head-on method delineates lateral changes in resistivity. Assuming that the Head-on data represents the subsurface structures without being affected by lateral changes in resistivity, a 2-D resistivity model was finally constructed.

The Krafla geothermal field may probably have a source of heat coming from the bottom since the magma body may lie at levels of about 3-7 km, (Einarsson, 1978).

And at the K_r 106 and 109, the 2-D resistivity model shows very conductive (5 Ωm) veins below the depth of about 300m surrounded by rather conductive (10-50 Ωm) zones; the very conductive (5 Ωm) and semi-conductive (10-50 Ωm) zones may possibly represent

permeable saturated hot fluids and impermeable saturated warm fluids zones, respectively. The 1-D resistivity model shows the presence of resistive bodies underlay the conductive zones as it is shown in Figure 8a. If it is the case, the reversed temperature profiles shown by the three wells at Hvitholar may indicate either outflow of thermal fluids having their source in Krafla or some places at Hvitholar. The latter one is not doubtful, (Eyjolfsson, pers. comm.). This interpretation may also be supported by the following evidences. Firstly, the westward outflow of thermal fluids interpreted from the pressures observation in the wells. Secondly, the lack of permeability and heat encountered at the south edge of the Krafla geothermal field. But, the following facts do apparently not support the interpretation, i.e., a) the observed resistivity (Schlumberger) data are restricted to probing depths of about 800 m (AB/2 = 1780 m), thus there is no information below that depth. And, b) the temperature measurements in the KJ-23 start apparently increasing at depth of about 1800 m; the well KJ-23 indicates high temperatures but poor permeability.

5. CONCLUSIONS

The Wenner and Dipole-dipole methods applied in New Zealand works well on relatively flat terrain where resistivities do not change abruptly. The Schlumberger method applied at the Hvitholar geothermal area did not delimit the area of the geothermal system since the lateral changes in resistivity occurs very rapidly. The Head-on method can delineate the structures where the saturated hot fluids present producing the high contrast in resistivities.

To get a good 2-D resistivity model both the Schlumberger and Head-on methods should be applied; the Schlumberger methods give a better resolution of vertical variations in resistivities and the Head-on method in lateral directions.

Contouring the conductive layers obtained from the Schlumberger method may not help much in delineating the geothermal area of interest.

The general view of the resistivity distributions over the wide area including Krafla geothermal field is required to determine the resistivity substructure at Hvitholar area a bit clear.

PART TWO

6. RELOCATING HYPOCENTERS OF MICRO-EARTHQUAKES MONITORED DURING JANUARY-JUNE, 1985, AT THE LAHENDONG GEOTHERMAL AREA

6.1. INTRODUCTION

This paper evaluates the results of micro-earthquakes monitoring during January to June 1985 at the Lahendong geothermal field, North Sulawesi, Indonesia. The hypocenters were originally calculated using a constant velocity model and S-P times. In this study, they were relocated using two computer programs, i.e. HYPOINVERSE (Klein, 1978) and Basic-Hypo, (Mendoza and Morgan, 1985). The former one, written in fortran language, was applied by using two different simulated crustal velocity models. These models were also used for the application of the latter program, written in basic language. However, since there were only four seismometers available at Lahendong, and the program needs more seismometers to accurately locate the events, the results are not presented in this report.

The aim is to delineate, if any, the differences between the original location and the relocation of events, and in addition to observe the relation between the seismicity and geothermal areas.

The geothermal prospects in Indonesia, are shown in Figure 14. The geothermal fluids which may be produced from these areas will be used to supply a power demand of about 300-350 MW_e, which should be on line by 1992, (Akil, 1975, and Finn, 1979).

6.2. REVIEW OF EARTHQUAKE MONITORING AT GEOTHERMAL AREAS

Geothermal systems are generally located in areas of tectonic activity, volcanism and seismicity. Evidences from earthquake studies indicate that the seismicity in geothermal areas is strongly influenced by the regional structures. For example:

a) the extension of the zone of destructive earthquakes in south Iceland, (Bjornsson and Einarsson, 1974), b) focal mechanism solutions of earthquakes monitored in the Geysers geothermal area, California, reflect the tectonics of the regional Coastal Range belt, (Bolt et al., 1968), and similarly, c) studies of micro-earthquakes in the Hengill geothermal area indicate a large percentage of tensile crack events, believed to be influenced by the regional structures of the volcanic zones. Micro-earthquake monitoring is a passive observation of naturally occurring seismic events with small magnitude, rather than the measurements of waves generated by explosions or other artificial means. The method has become widely used in geothermal exploration. Einarsson (1978), studied the attenuation of S-waves through a shallow (3-7 km) body, which he suggested that was a magma chamber at Krafla geothermal field; this anomalous attenuation was not observed at similar depths (V_p = 6.5 km/s) across the volcanic rift zone in N-E Iceland. A distribution of hypocenters studied by Foulger (1984), was interpreted to shows two major heat sources for the Hengill geothermal area: the extinct Grensdalur volcanic centre and the active Hengill volcanic centre. However, the pattern of local earthquakes at the Fly-Ranch, Canada, did not conform well to the pattern of existing faults, (Kumamoto, 1978). The passive seismic method appears to be most effective in locating heat sources at deep levels, for example, in areas such as Krafla or Hawaii, were geothermal systems are associated with magma chamber within 2-3 km depth, (Einarsson, 1978, and Peck et al., 1968), but less so in mapping near surface features.

6.3. GEOLOGICAL AND GEOPHYSICAL BACKGROUND

6.3.1. Geological Setting

The Lahendong geothermal area is within the volcanic country of Minahasa which lies in the inner arc, extends to the Sangihe volcanic islands in the north and continues on to the Philippine archipelago, (Bemmelen, 1949, and Hamilton, 1979). The Neogene

pyroclastic rocks are overlain by Quaternary volcanics consisting of andesitic lava, breccia and welded tuff, (Kartijoso, 1982). Most of the lavas are brecciated and some of them hydrothermally altered. Within the Lahendong geothermal area there is a caldera. At present, the depression inside the caldera is filled with the acid water from which the name of the Lake Linau comes; linau means acid.

6.3.2. Geophysical Exploration

Schlumberger resistivity sounding profile conducted at the Lahendong area, (Marino, 1977), showed a shallow conductive (2.5-5 Ωm) zone underlain by resistive (is higher than 10 Ωm) substratum and located between two resistive zones. This conductive zone was interpreted that may probably indicate hot water saturated rocks. Since then, intensive geophysical, geochemical, and geological surveys have been conducted in order to find a viable deep geothermal reservoir. The results of geochemical survey were used to infer that the Lahendong geothermal area could probably be a hot water dominated system. Studies of deep exploration wells indicate the upper reservoir encountered at levels of about 400 and 800 m contains acidic water with temperatures of about 260°C. The bottom reservoir below about 1500 m has neutral pH fluids with temperatures of about 330°C, (Surachman et al., 1985).

6.4. EQUIPMENT AND DATA PROCESSING

6.4.1. Equipment

Four seismometers, type M.E.Q.-800 with vertical geophones model L-4C, made by Sprengnether were used to monitor the micro-earthquakes at Lahendong geothermal area. These were also equipped with a time-cube model TS-400 to synchronize the time during monitoring every two days (48 hours).

6.4.2. Locating The Micro-Earthquakes

The hypocenters were originally calculated using the relationships in the following formula, (PERTAMINA, 1985):

$$d = (t_s - t_p) * (V_p * V_s)/(V_p - V_s) \qquad (2)$$

where :
d - distance of the event from the seismometer in km,
V_p - velocity of the longitudinal wave in km/s,
V_s - velocity of the shear wave in km/s,
t_p - arrival time of the longitudinal wave in s,
t_s - arrival time of the shear wave in s.

The distance of the event from each seismometer (d) can be calculated since the ratio of $(V_p * V_s)$ to $(V_p - V_s)$ is established. The ratio of 7.5 km/s was used to calculate the hypocenters due to Lahendong's crustal structure similarity to the Dieng geothermal field, Central Java, where laboratory measurements of wave velocities in cores sampled from the wells and the surface are available. For comparison, average regional velocities in the upper crust are estimated to be 5.39 km/s and 2.93 km/s respectively for the P- and S- waves, (Hars et al., 1980), giving a ratio of about 6.42 km/s.

In this study, the events were relocated using the hypocentre location program HYPOINVERSE by Klein (1978). The upper part of the crustal velocity model involving layers with linear gradient was estimated by comparison with the crustal velocity model of Matsukawa geothermal field in Japan, (Baba et al., 1970), while the middle and lower part were merely estimated by assuming that the velocity at depth of about 5-15 km and below 30 km are about 5-6 and 8.1 km/s, respectively. Matsukawa was used due to its lithological and structural similarities with Lahendong geothermal area. The model was then varied somewhat to see how it affected the resulting locations. These two models are tabulated in Table 1, and plotted in Figure 18 which also shows travel times calculated for a surface source.

A second location program, the Basic-Hypo, written in basic language (Mendoza and Morgan, 1985), and recently available at the UNU Geothermal Training Programme in Iceland, was also used to calculate these events. However, since there were only four seismometers available at Lahendong as shown in Table 2, and the Basic Hypo program needs more seismometers to accurately locate the events, the results are not included. While the Hypoinverse does not need as many seismometers as the Basic-Hypo, it still requires that at least four arrival times be input in the computer. Therefore, only events which were recorded by all four seismometers were included in this study. These were about 167 out of 500 events (PERTAMINA, 1985).

6.4.3. Magnitude

Magnitudes of all of the events were calculated using the following formula, (Butler, 1979):

$$M = \log A - \log A_0 + \log A_{20} + \log (2800/G)$$

where,
M - Magnitude of the events,
A - Amplitude of reference earthquake,
G - Gain of the earth displacement at 20 H_z,
$\log A_0 = 1.6 * \log D - 1.55$,
$\log A_{20} = 0.11$ D, and
D - Depth of micro-earthquake.

6.5. RESULTS

The events are in the magnitude (analogous to Richter magnitude) range from 0.4 to 3.5. About 80% of the events occurred at depths down to 9km.

The relocation of events which were calculated using the first crustal velocity and the second model, are plotted on Figure 16 and 17, respectively. The epicenters calculated from the

first model, were displaced dramatically from the original ones, see Figure 15 and 16. However, no obvious displacement of events occur due to the change from the first to the second model, as shown in Figures 16 and 17. All three maps, however, indicate that epicenters cluster outside the caldera rim within the area of 125°50-55' and 1°15-20', and only a few are located inside the caldera rim. The distribution of events on the surface does not correlate well with existing faults. The focal depths of the events calculated by using the first and the second model also showed slight displacement as is observed for epicenters locations, and these are absolutely displaced from the original ones, see Figures 19 and 20. The events surrounding the caldera rim are mostly shallow as they may be observed in detail in E-W and N-S sections crossing the densest events, see Figure 19 and 20.

6.6. DISCUSSIONS

From the data presented here, the micro-earthquakes are significantly concentrated outside the caldera. Only few events were located within the caldera rim. Two models of the heat source of the geothermal system at Lahendong could be postulated to explain the phenomenon :

First model :
The hot rocks rest in the region and are cooled from the outside by meteoric water. The location of the hot rocks may be supported by the appearance of thermal manifestations. Hence, the seismicity is due to the contraction and subsequent fracturing induced by cooling hot rocks; meteoric water comes into contact with hot rocks. Low activity inside the caldera may mean that the cooling front has not reached this part yet.

Second model :
The hot rocks lay at very deep level inside the caldera. The heat is carried out vertically by meteoric waters forming hot geothermal fluids.

On the way to the surface, the hot fluids flows out towards the north east, and comes into contact with cool rocks. Hence fracturing occurs to induce the seismicity. The low activity inside the caldera is caused by regional strain released aseismically within the caldera because of very high temperature which may reach at least 400°C within a few km from the surface. The temperature about 350°C has been encountered in the wells at depth of about 2km at Lahendong and at the other hot water dominated system geothermal fields, e.g. Lahendong, Dieng and Salak (Indonesia).

The diagram of number of events with depth shows increasing number of events down to 3km and a decrease in number of events below. This similar form of the diagram is also seen in other seismic areas but the peaks occur at larger depth, from 5 to 10 km, (Meissner and Strehlau, 1982). The shallow peak at the Lahendong ma possibly be because of high heat flow here.

There is no clear evidence indicating a fault-like structural plane in the E-W and N-S focal depth sections shown in Figures 19 and 20. But the rather dense events located near the caldera shown in Figure 20a may possibly be due to a faulting zone at depth.

A plot between the magnitudes and number of the events is not presented in this report, since the number of events was only about 35 % out of the total events.

6.7. CONCLUSIONS

All of the results are still open to question, since they depend on crustal velocity models. The first velocity model was chosen for Lahendong geothermal area, due to its structural similarity to the Matsukawa geothermal area, Japan.

The locations of events seemed not to be affected by small changes in the velocity model.

Two models of mechanism remain plausible for inducing seismicity at Lahendong. Firstly, volumetric contraction due to the contact between hot rocks and cool fluids, or vise versa, and secondly, fracturing induced by the regional tectonic activity.

The maximum number of events was found at the depth of 3km. If the events are caused by the volumetric contraction due to the contact between hot rocks and cool meteoric water, then at this depth it may reflect the fracture zones where the geothermal reservoir exists, otherwise reflecting high heat flow.

6.8. SUGGESTION

An seismic explosion survey should be done as soon as possible which may refine the crustal velocity model, presented in the report, at Lahendong geothermal area. More seismometers should be used in monitoring micro-earthquakes to ensure the accuracy of the results and to study focal mechanisms besides. The additional seismometers in the area of dense events will better constrain their focal depth.

To remove some of the uncertainty about the model of the geothermal system at Lahendong, it may be worth drilling in the area of the dense events. If the first model is correct, a zone of high rate of heat exchange may encountered.

ACKNOWLEDGEMENTS

The author would like to acknowledge National Energy Authority and PERTAMINA Managements for permission to publish the data in this report. My grateful thanks are extended to Dr Brynjolfur Eyjolfsson and Dr Pall Einarsson for supervising, reading, correcting the manuscript and making many valuables suggestions for its improvements.

Special regards to Dr Jon Steinar Gudmundsson, the director of the United Nations University Geothermal Training Programme, for his guidance and valuable advice.

I am also indebted to Mr Sigurjon Asbjornsson, Mr Bessi Aðalsteinsson, and Miss Anna Maria Sverrisdottir, staff of UNU Geothermal Training Programme, and Miss Olafia, land-lady, for taking care during attending the Geothermal Training Programme in Iceland.

REFERENCES

Akil, Ismet, (1975) : Development of Geothermal Resources in Indonesia. Proceedings of the Second United Nations Symposium on the Development and Use of Geothermal Resources, Vol. 1, 11-15.

Al'pin, L. M., (1950) : The theory of dipole sounding. English translation, Geotoptekhizat.

Armansson, Gislason, H.,G., Hauksson, T., V., (1982) : Magmatic gases in well fluids aid the mapping of the flow pattern in a geothermal system. Geochim., Cosmochim. Acta, 46.

Arnason, K., Eyjolffsson, B., Gunnarsson, K., Sæmundsson, K, Björnsson, A., (1984) : Krafla - Hvitholar, Jarðfræði og jarðeðlisfræðikönnun, 1983. OS-84033/JHDö04, Reykjavik.

Baba, K., S. Takai, G. Matsuo, and K. Katagiri, (1970) : On the reservoir at Matsukawa geothermal field. United Nations Symposium on the development and utilization of geothermal resources. Section VII, reservoir physics and production management, VII/11, Sept. 28, Pisa.

Bemmelen, R., W.,Van, (1949) : The geology of Indonesia. Gov. Printing Office, Martinus Nijhoff, The Hague, Nederland, Vol. IA.

Björnsson, S. and Einarsson, P., (1974) : Seismicity of Iceland. Geodynamics of Iceland and the North Atlantic Area (Edited by Kristjansson, L., D.), 225-239. Reidel, Dordrecht, Holland.

Bolt, B. A., Lomnit, C., and Mc Evilly, T. V., (1968) : Seismological evidence on the tectonics of central and northern California and Mendocino escarpment. Bull. Seim. Soc. Am. 58, 1725-1767.

Butler, D., (1979) : Notes on Seismic for geothermal energy. Microgeophysics Corporation, Colorado, U.S.A.

Cheng, Y.W. (1980) : Location of near surface faults in geothermal prospects by "Combined head-on resistivity profiling method". Proceeding of the New Zealand Geothermal Workshop.

Einarsson, P., (1978) : S-wave shadows in the Krafla caldera in NE-Iceland, evidence for a magma chamber in the crust. Bull. Volcanol., Vol. 41-3.

Finn, D. F. X., (1979) : Geothermal Developments in the Republic of Indonesia - 1979. Geothermal Energy Institute. Geothermal resources Council, TRANSACTIONS, Vol.3., September.

Foulger, G. R., (1984) : The Hengill Geothermal Area : Seismological Studies 1978-1984. Science Institute University of Iceland, Dunhaga 3, 107 Reykjavik.

Hamilton, W., (1979) : Tectonics of the Indonesian Region, Geological Survey Profess. Paper, 1078, pp. 159-189.

Hars K. Gupta, Tzeu-Lie Lin, and Ronald W. Ward, (1980) : Investigation of Seismic Wave Velocities at the Geysers Geothermal Field, California. Geothermal Resources Council, vol. 4.

Kartijoso, S., (1982) : Borehole geology of well Lh-2 Lahendong High Temperature area, N- Sulawesi, Indonesia. UNU Geothermal Training Programme, Iceland, report 1982-11.

Keller, G., V., and Frischknecht, F., C., (1966) : Electrical methods in geophysical prospecting. Pergamon Press, New York.

Klein, F., W., (1978) : Hypocenters location program inverse. U.S.G.S., Open file report, 78-694.

Koefoed, O., (1979) : Geosounding Principles, 1. Elsevier Scientific Publishing Company, Amsterdam, Oxford, New York.

Kumamoto, L., (1978) : Microearthquake survey in the Gerlach Fly Ranch area of north-western Nevada. Quterly, Colo. School of Mining, in press.

Marino, (1977) : Penggunaan cara tahanan jenis dan gaya berat pada eksplorasi Panasbumi didaerah kenampakan panasbumi, Lahendong, Tompaso, Sulawesi Utara. Lang. Bhs Indonesia. Unplub., Geol. Survey Indonesia Report.

Meissner, R., and Strehlau, J., (1982) : Limits of stresses in continental crusts and their relation to depth-frequency distribution of shallow earthquakes. Tectonics, vol. 1, 73-89. American Geophysical Union.

Mendoza, J., and Morgan, D., (1985) : Basic-Hypo. A Basic language Hypocenter location program user's guide. School of earth sciences. Stanford University publications, Stanford, Geological Sciences, Vol. XIX, number 1.

Peck, D., L., and Minakami, T., (1968): The formation of columnar joints in the upper part of Kilaulan lava lakes, Hawaii, Geol. Soc. Amer. Bull., 79, 1151-1166.

PERTAMINA, (1985) : Pengamatan gempa mikro di daerah Lahendong, Sulawesi Utara. (" Micro-earthquakes monitoring at the Lahendong area, North Sulawesi"). Internal report. Unpubl.

Risk, G. F., Macdonald, W.J.P., and Dawson, G.B., (1970) : D.C. Resistivity Survey of the Broadlands Geothermal Region, New Zealand. Geothermics (1970) - Special Issue ; U.N. Symposium on the Development and Utilization of Geothermal Resources, Pisa, Vol.2, Part I.

Sigurdsson, O., Steingrimsson, B., S., and Stefansson, V., (1985) : Pressure build up monitoring of the Krafla geothermal field, Iceland. Tenth workshop on Geothermal Reservoir Engineering, Stanford University, Jan., 22-24.

Sigurdsson, R., (1986) : Lecture at the Geophysical section, National Energy Authority, Iceland.

Surachman, S., Tandirerung, S., A., and Robert, D., (1985) : Preliminary results and future promises for the development of the Lahendong geothermal field, North Sulawesi, Indonesia. Pertamina internal report, for publ., in prep.

Wale, A., 1985 : Reservoir engineering study of the Krafla-Hvitholar geothermal area, Iceland. UNU Geothermal Training Programme, Iceland. Report 1985-10.

Model	Velocity, km/s	Depth, km
First	2.50 5.00 6.00 8.10	0 2.50 15.00 30.00
Second	3.00 5.50 6.00 8.10	0 9.00 15.00 30.00

Table 1. Attempted crustal velocity models used to calculate the hypocenters of micro-earthquakes monitored during January - June, 1985, Lahendong, Indonesia.

Station No.	Longitude E	Latitude N	Elev. (a.s.l., m)
41	124° 46' 40''	1° 16' 15''	600
42	124° 49' 53''	1° 14' 28''	700
43	124° 52' 22''	1° 15' 08''	800
44	124° 50' 52''	1° 19' 20''	700

Table 2. Shows coordinates of the seismometer locations.

Figure 1. The electrode array of Sclumberger.

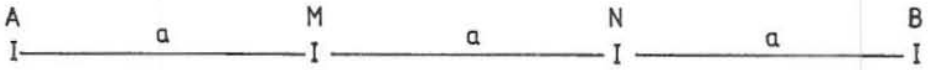

Figure 3. The electrode array of Wenner.

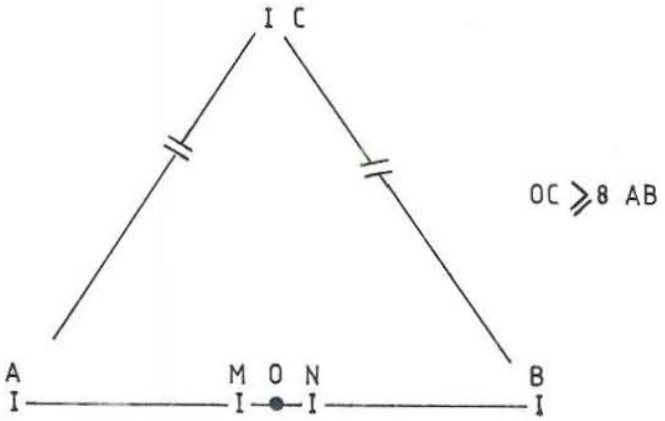

Figure 2. The electrode array of Head-on.

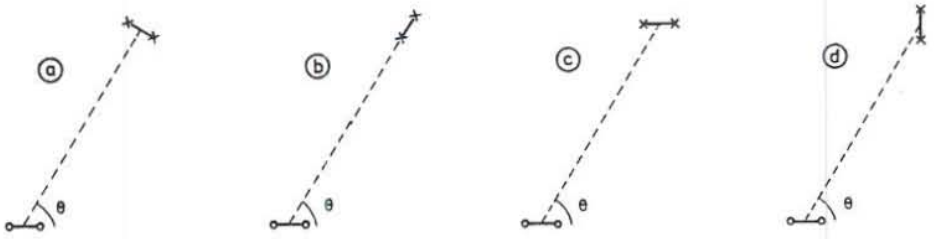

Figure 4. The electrode array of dipole-dipole, a) azimuthal, b) radial, c) parallel, and d) perpendicular.

a.

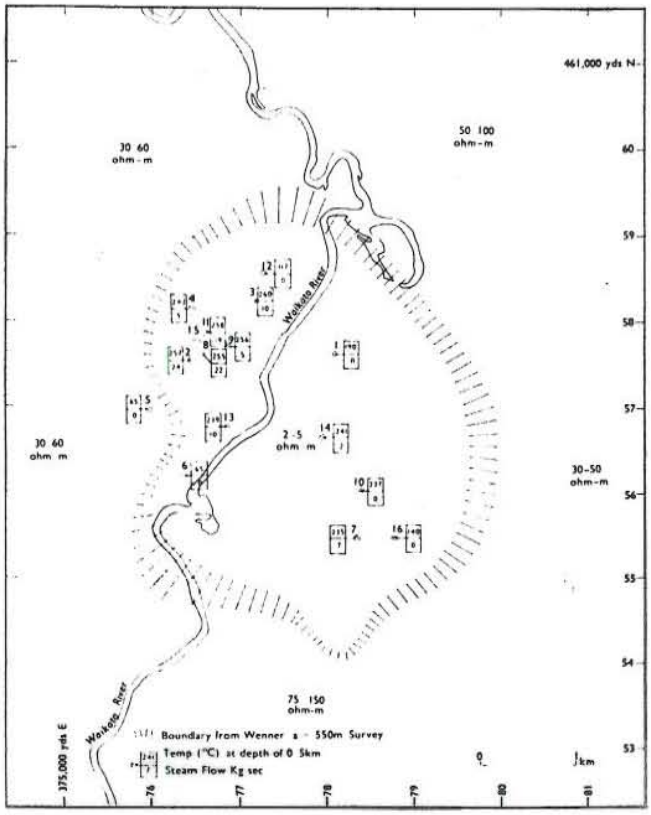

b.

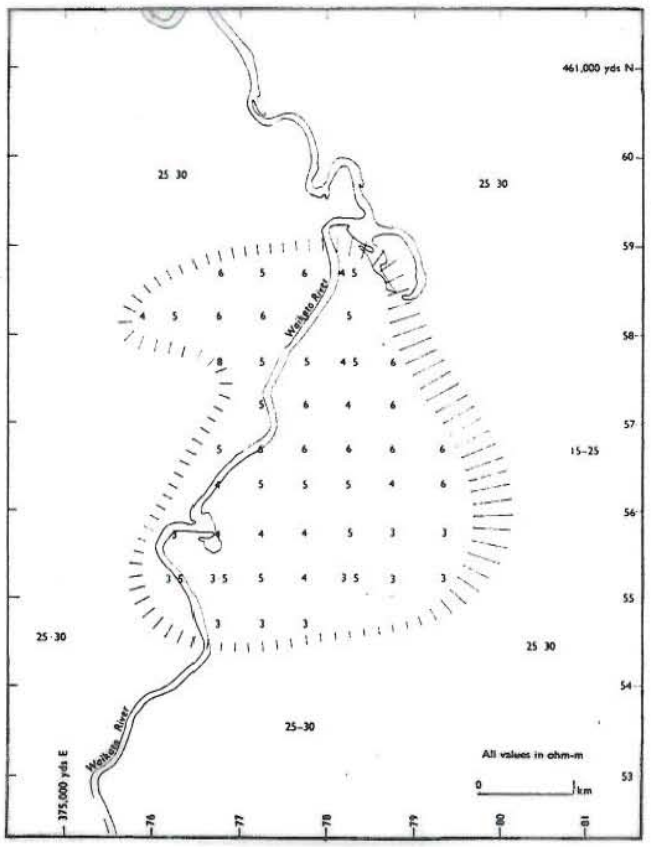

Figure 5. Geothermal field boundary , Broadlands, New Zealand.
a) by applying Wenner method with a=550m, and
b) dipole-dipole method.

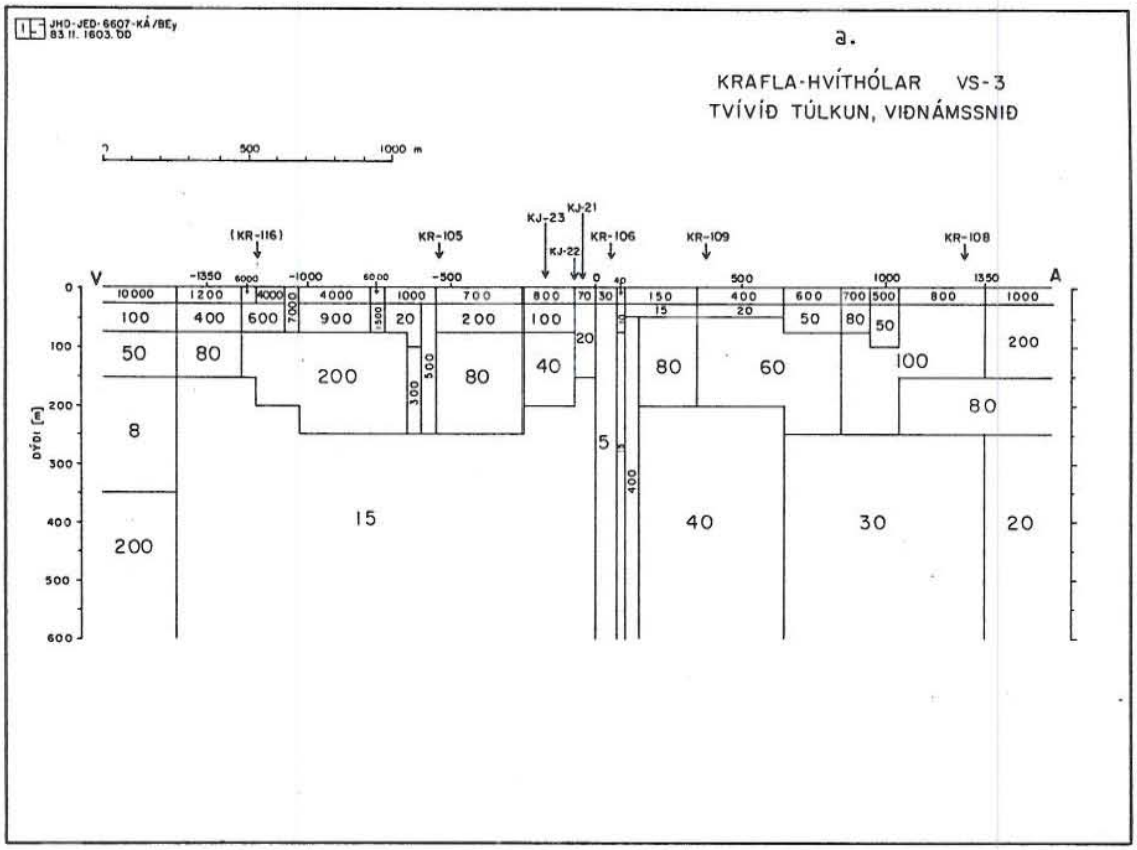

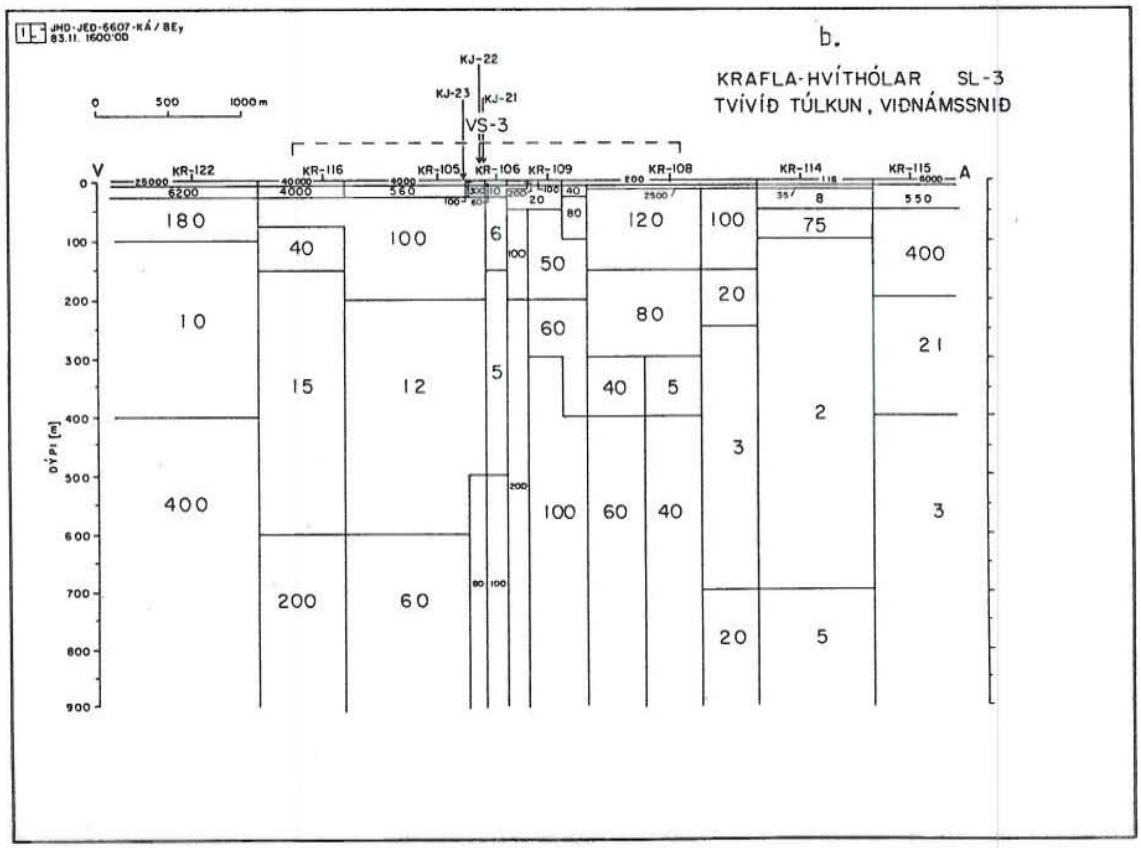

Figure 6. 2-D resistivity model of Hvitholar geothermal area, E-W section, constructed from : a) Head-on and b) Schlumberger methods, (Knutur Arnason et al., 1983).

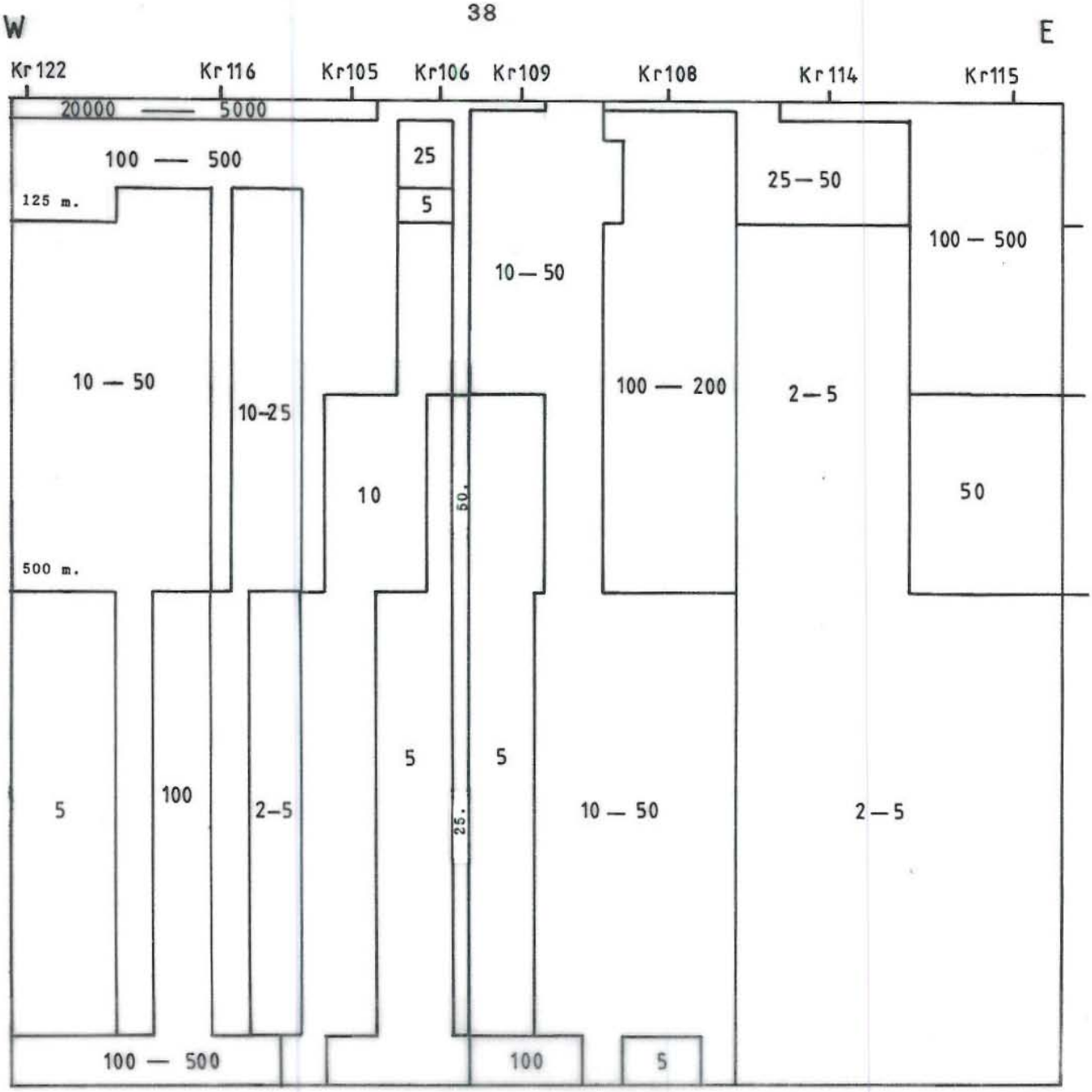

Figure 7. 2-D resistivity model of E-W section, Hvitholar geothermal area, constructed from the combination the Schlumberger and Head-on method.
The location of soundings are in Figure 10 and 11.

Kr 122 Resistivity sounding station.

Head-on resistivity profiling.

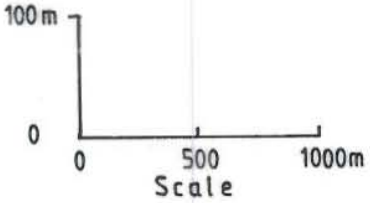

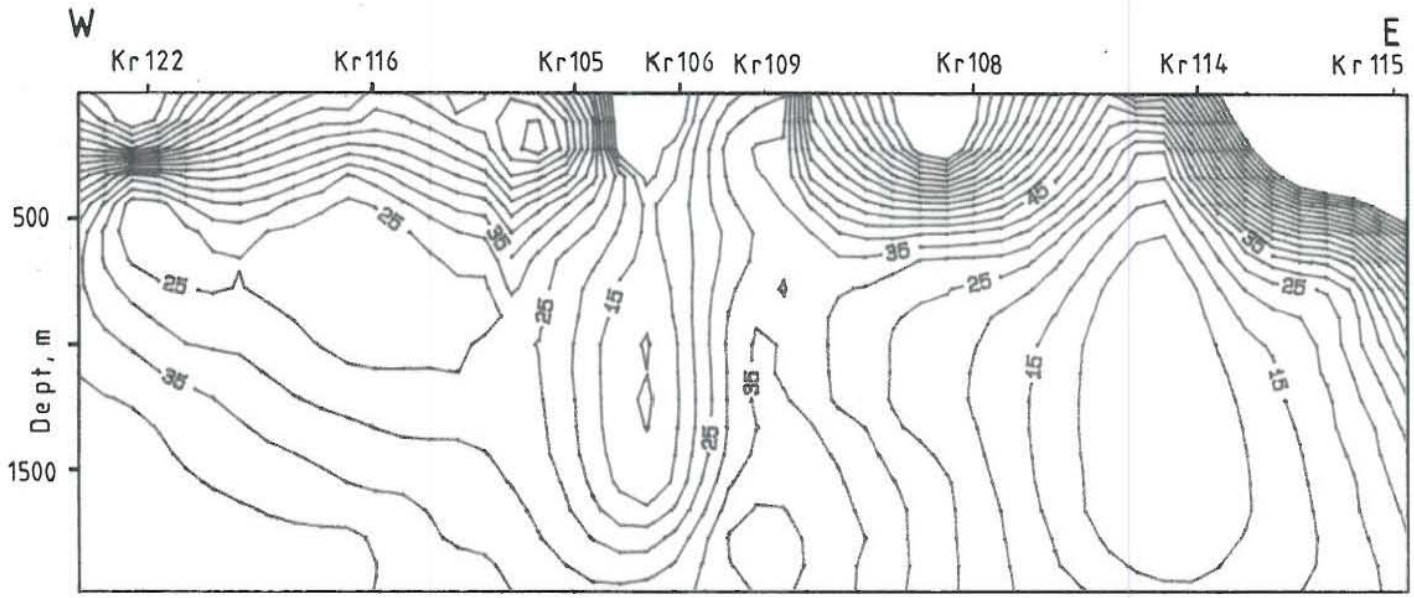

Figure 8a. Contour of observed apparent resistivities (Schlumberger), E-W section, Hvitholar, Iceland.

. Kr 122 - Resistivity sounding station.

15 - Resistivity contour line in Ωm.

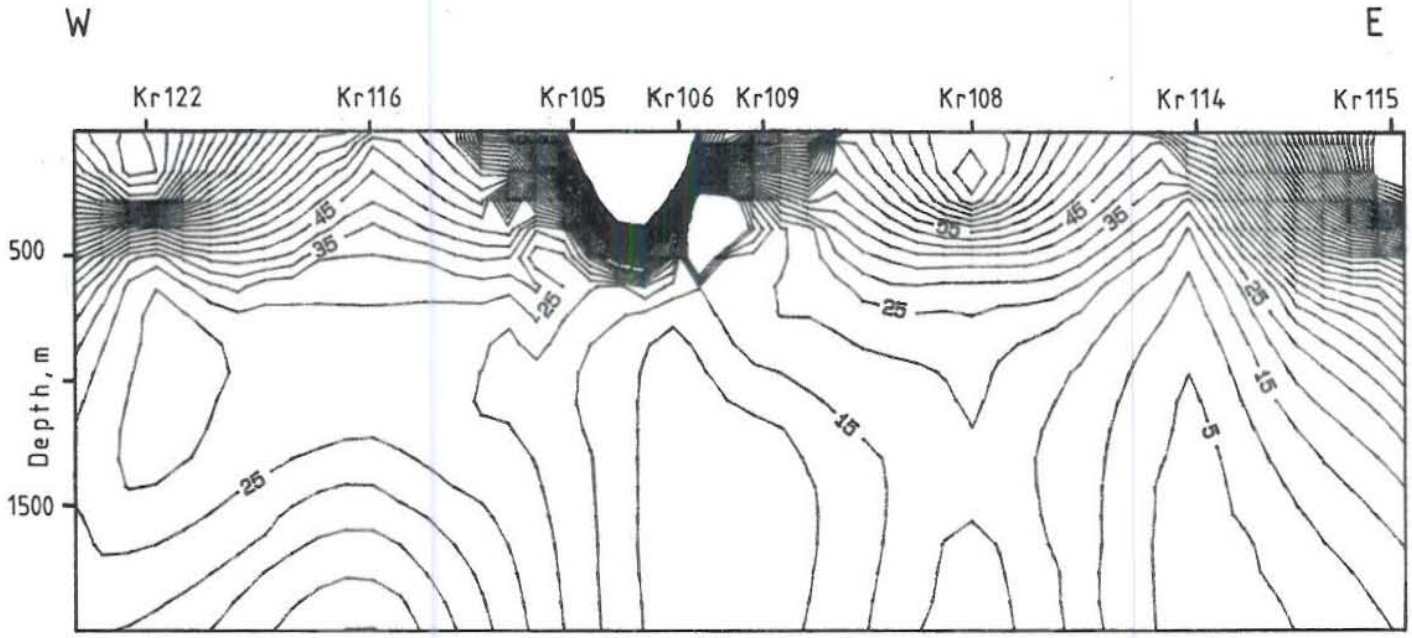

Figure 8b. Contour of apparent resistivities (Schlumberger) calculated by using 2-D resistivity model of E-W section, Hvitholar, Iceland.

. Kr 122 - Resistivity sounding station.

15 - Resistivity contour line in Ωm.

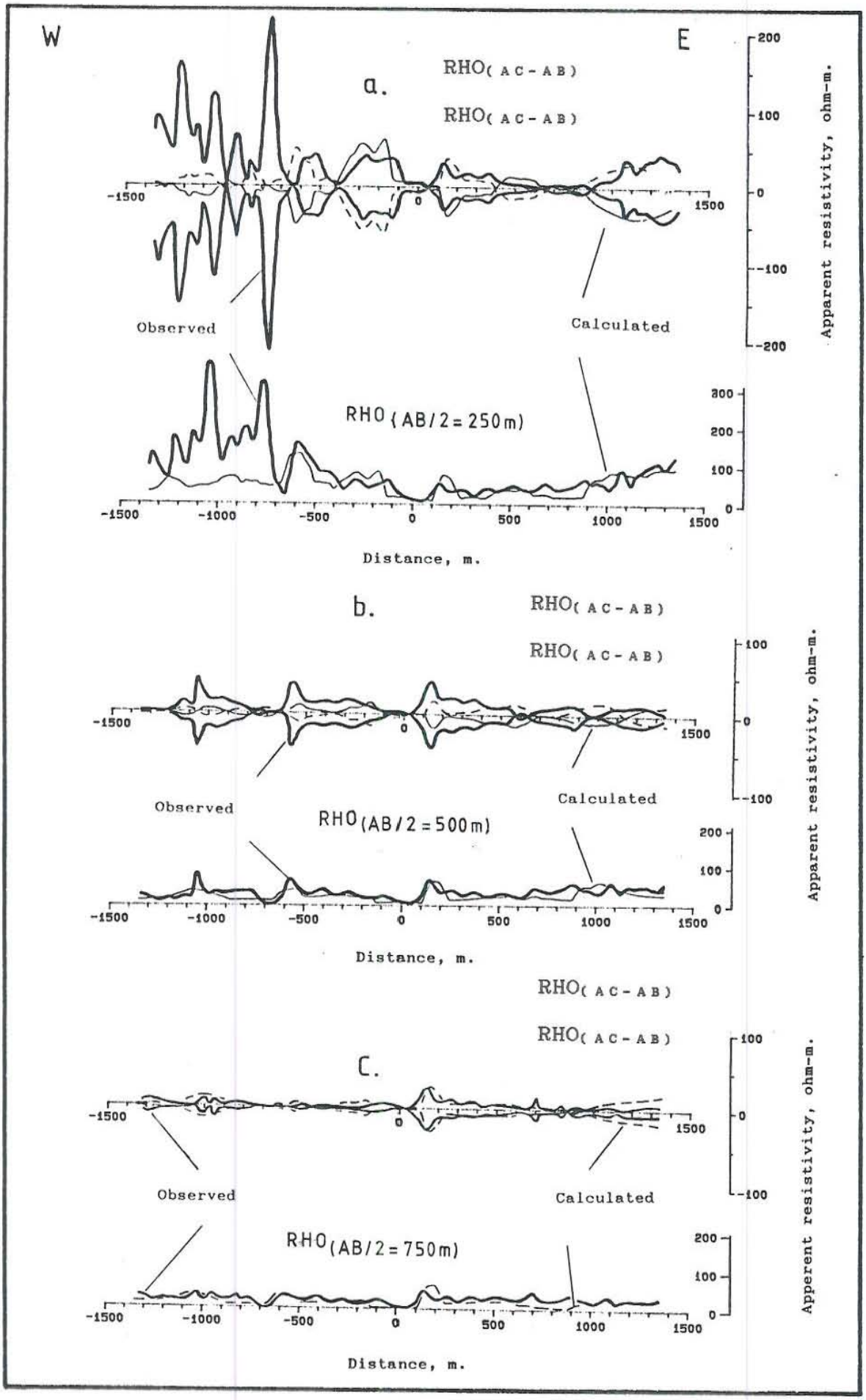

Figure 9. Apparent resistivities of Head-on method, observed and calculated by using 2-D resistivity model, E-W section, Hvitholar, Iceland.

a) For AB/2=250m, b) 500m, and c) 750m.

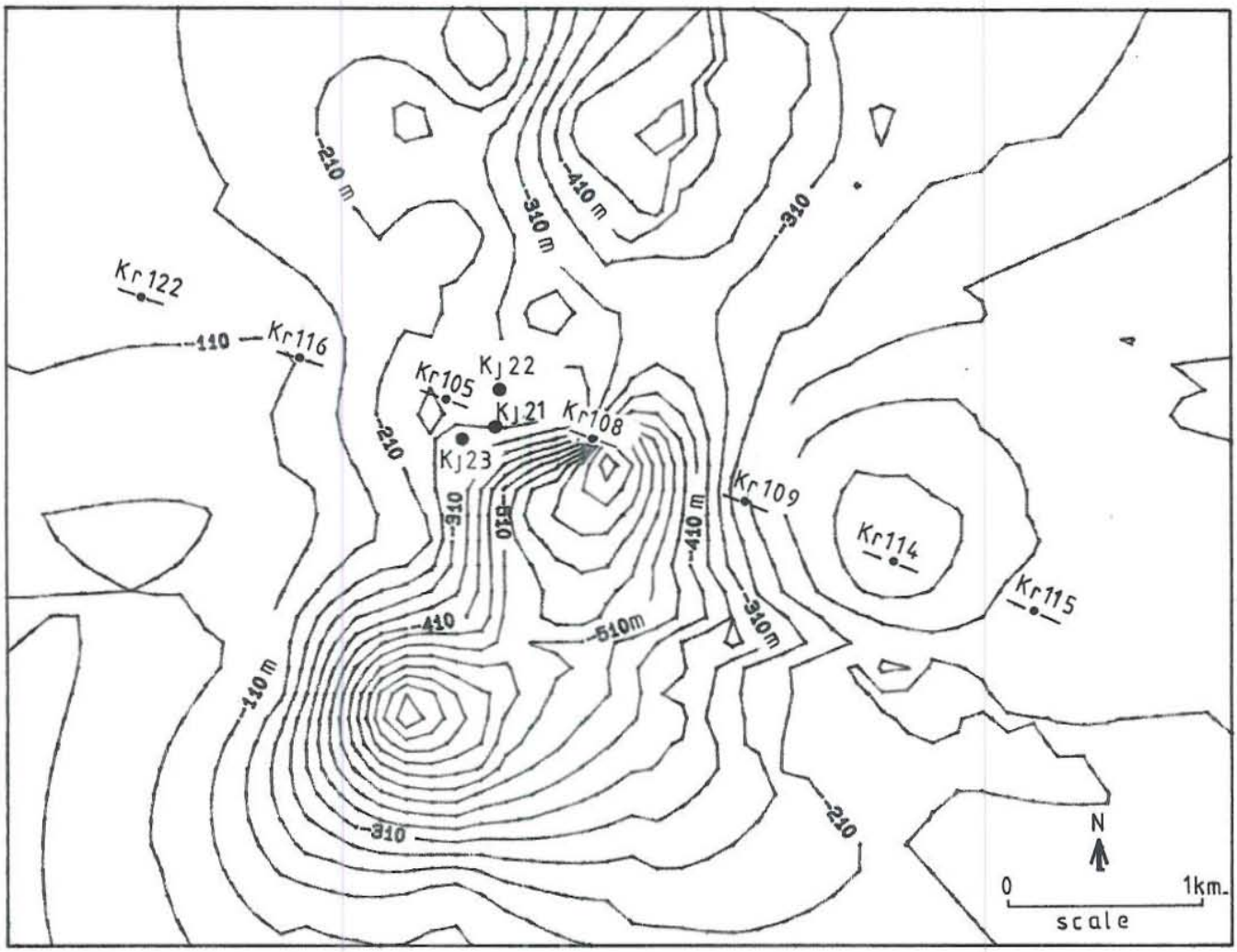

Figure 10. Map showing top conductive (≤ 20 Ωm) layers at the Hvitholar geothermal area, Iceland.

Kj 21 ● Geothermal exploration well.

Kr 108 Resistivity sounding (Schlumberger) Kr108, used to constuct 2-D resistivity model.

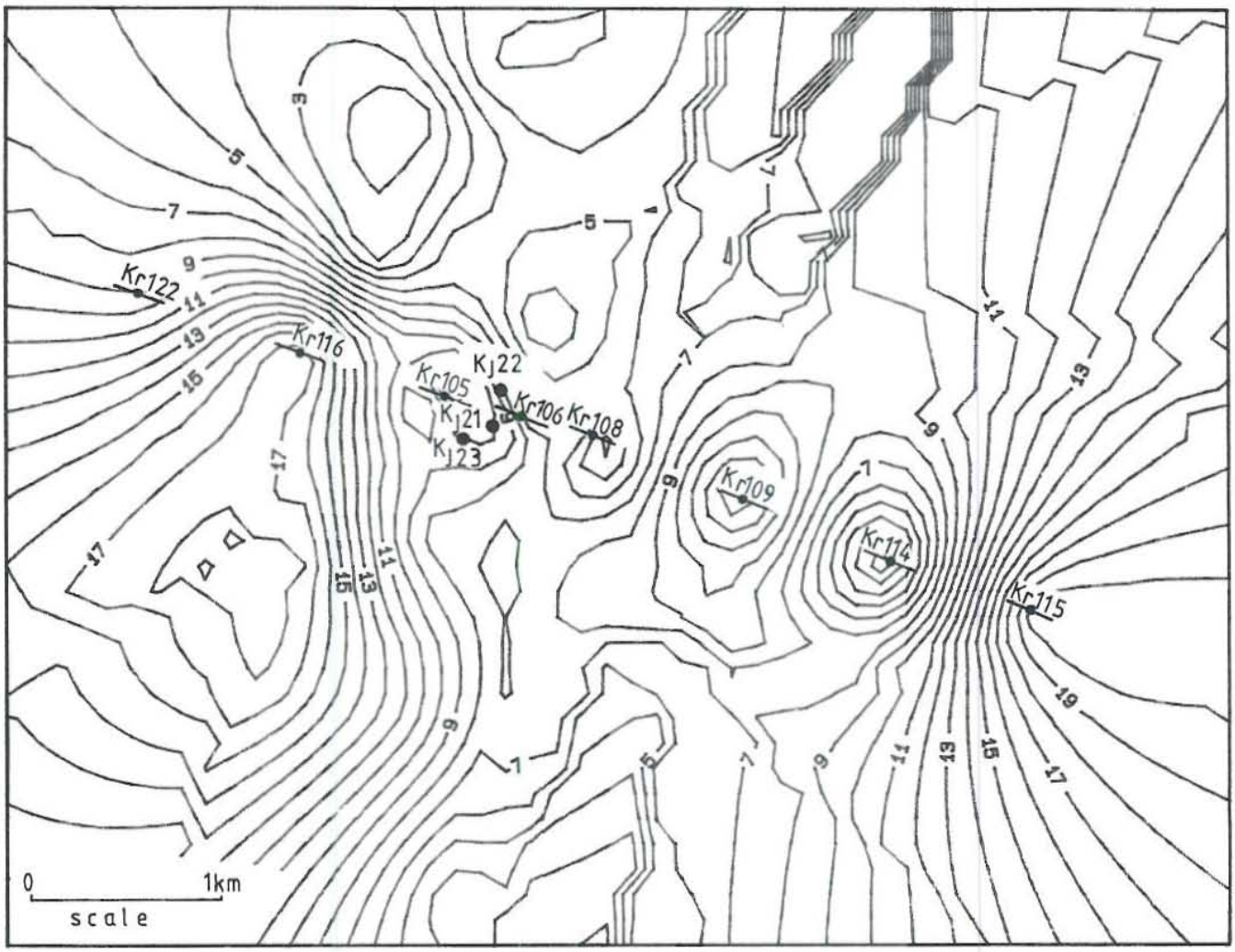

Figure 11. Map showing the resistivity variations (Ωm) within the conductive layers, Hvitholar, Iceland.

Kj 21 ● Geothermal exploration well.

Kr 108 Resistivity sounding (Schlumberger) Kr108, used to construct 2-D resistivity model.

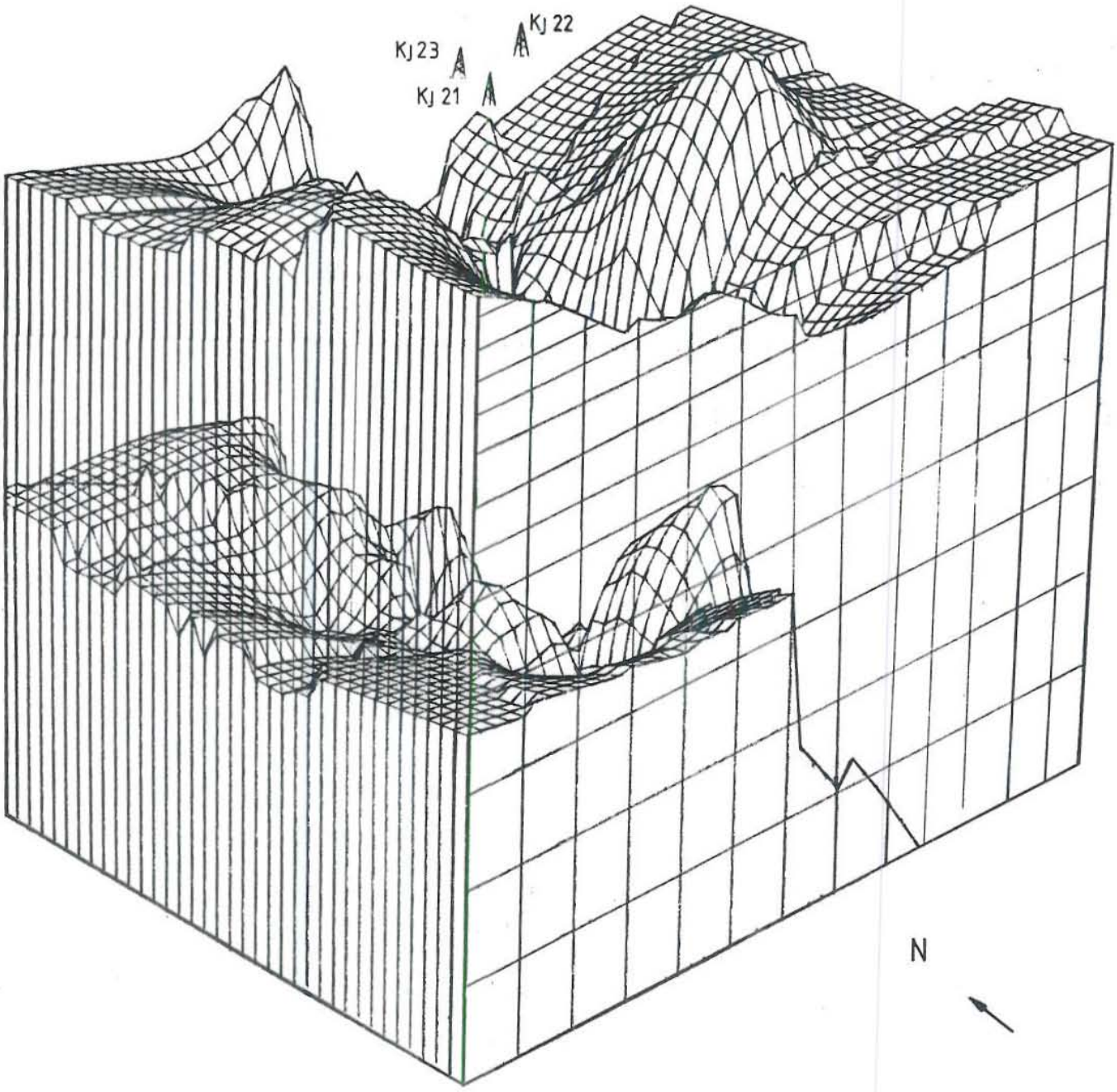

Figure 12. Shows top conductive layers in perspective viewing at angles of tilt and rotation of 30° and 225°, respectively, Hvitholar, Iceland. The locations of wells are approximated.

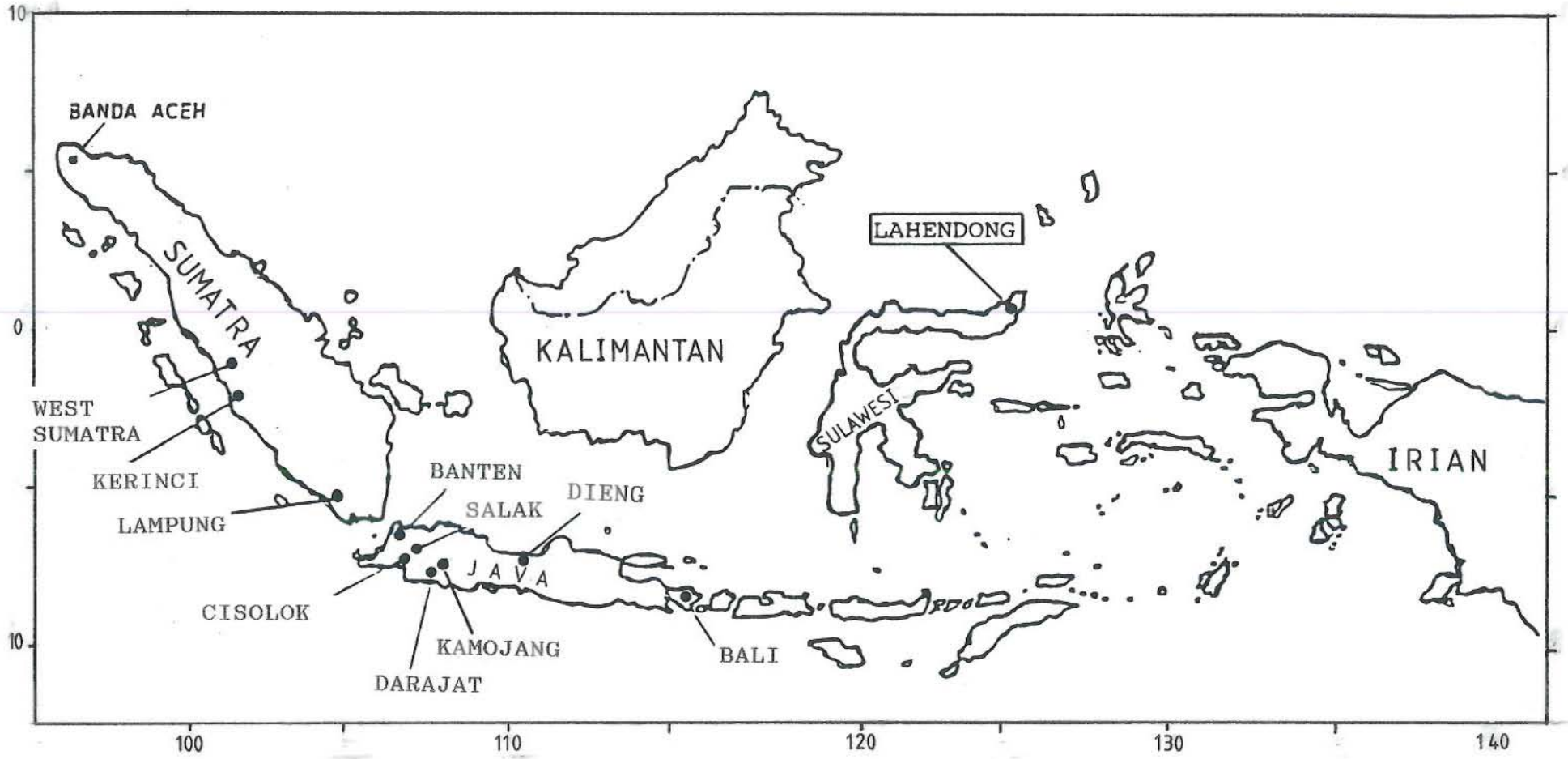

Figure 14. Map of Indonesia showing the identified geothermal prospect areas.

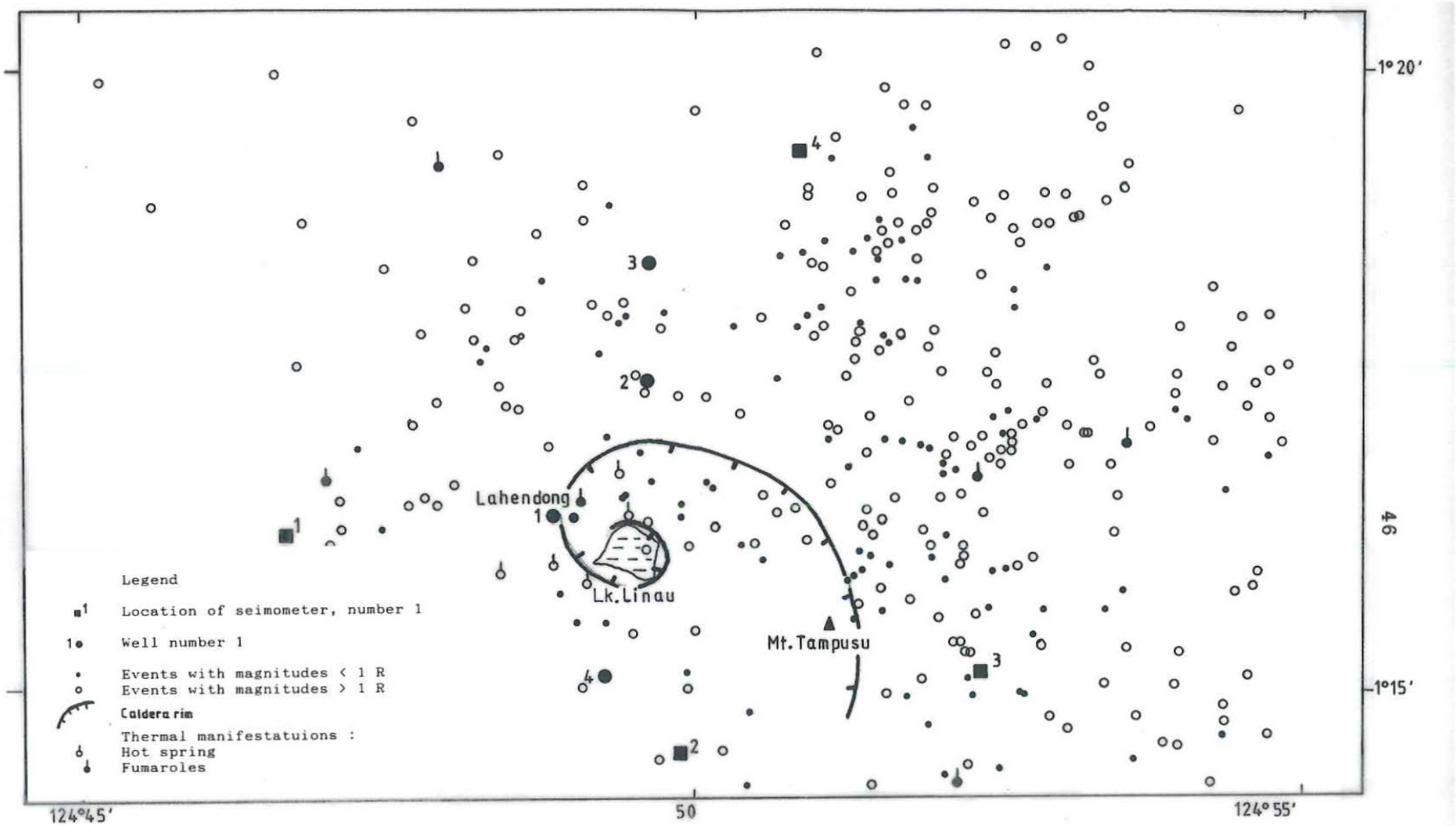

Figure 15. Map showing original hypocenters calculated by using single layer velocity model (equation 2), Lahendong, (PERTAMINA, 1985).

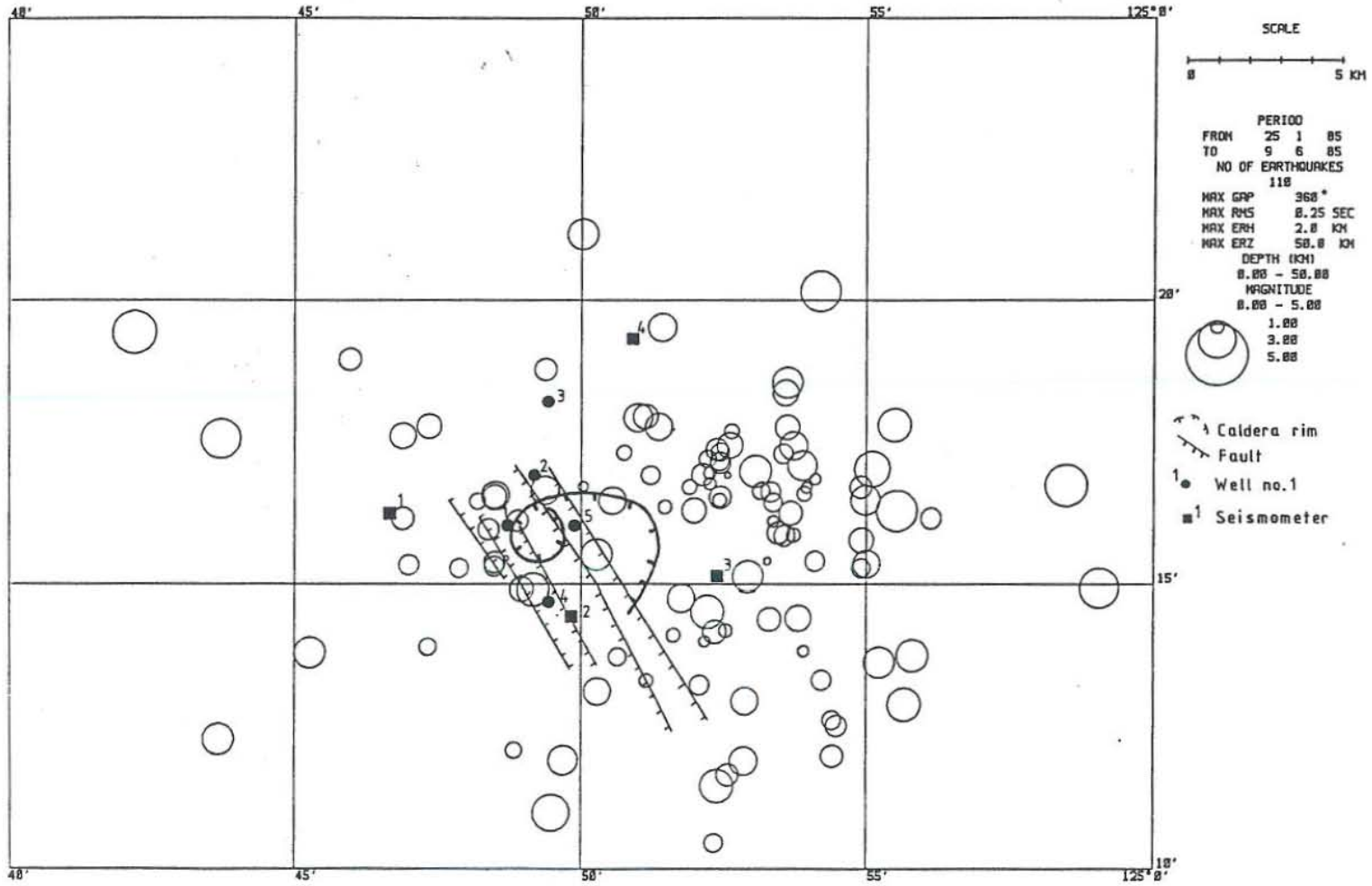

Figure 16. Map showing hypocenters recalculated by using the first crustal velocity model, Lahendong.

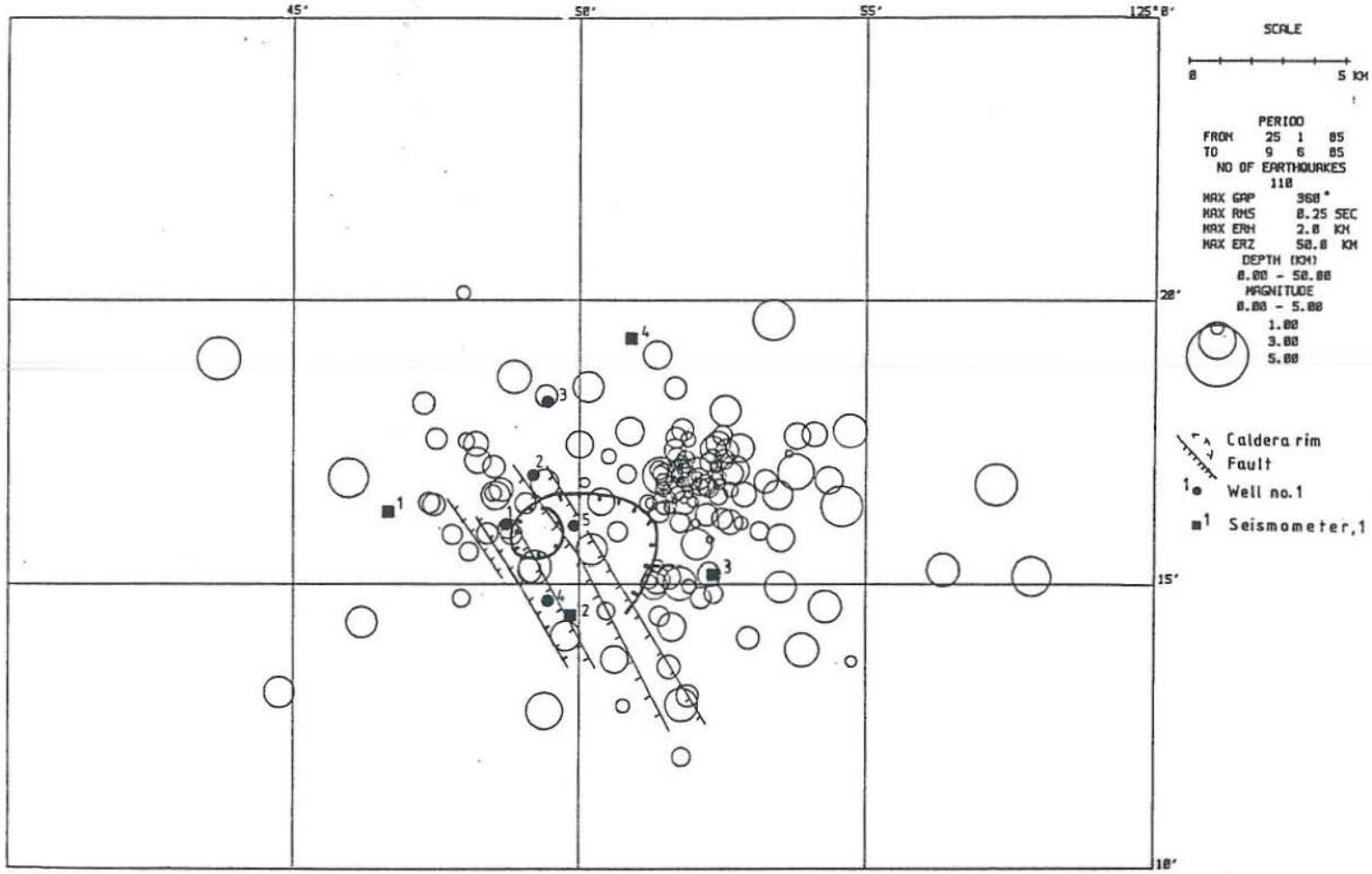

Figure 17. Map showing hypocenters recalculated by using the second crustal velocity model, Lahendong.

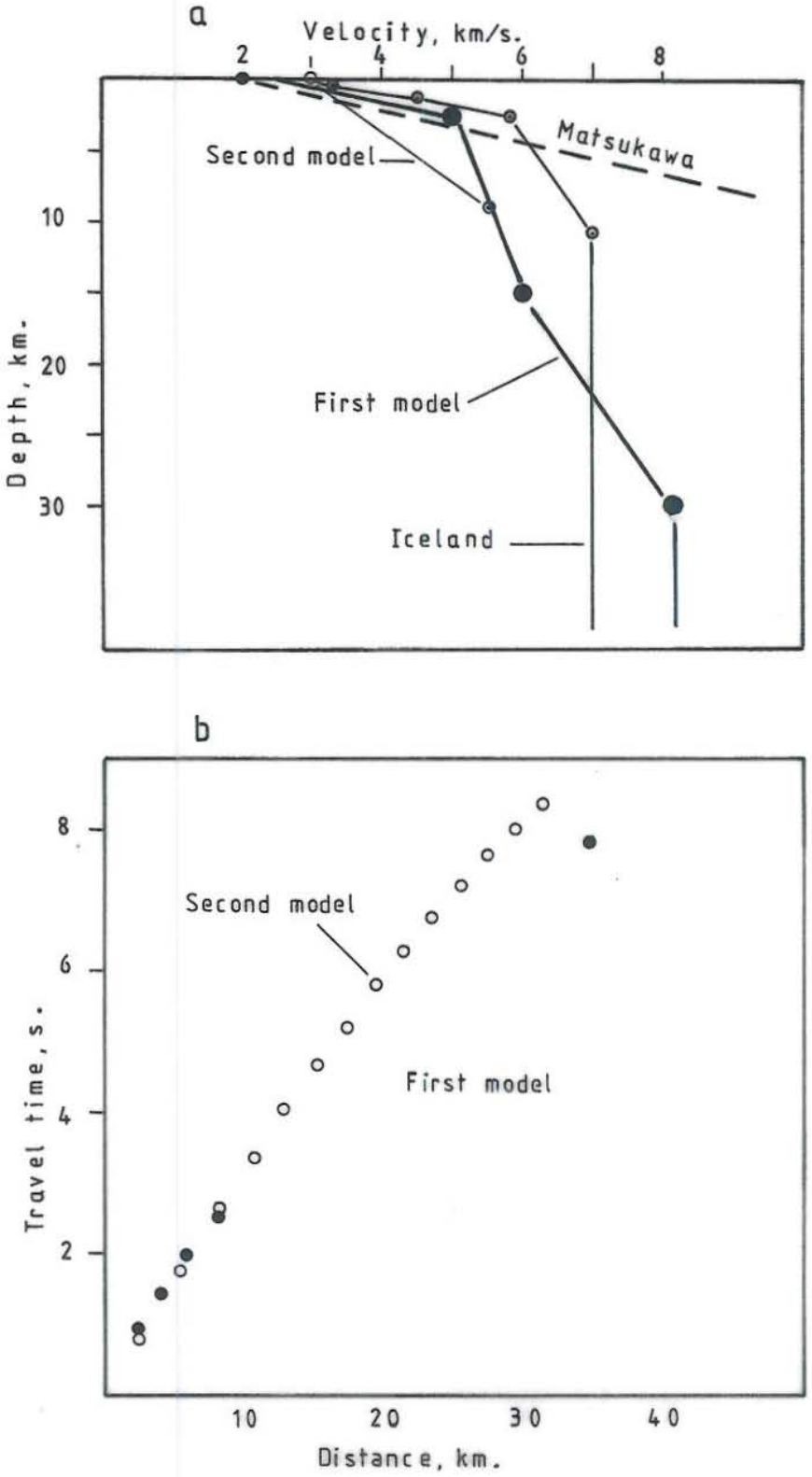

Figure 18. a) Plot velocity (km/s) Vs depth(km) showing models used in this study (first and second model), Iceland, and Matsukawa (Japan).

b) Plot travel-time (s) Vs distance(km) showing travel-time calculated for a surface source.

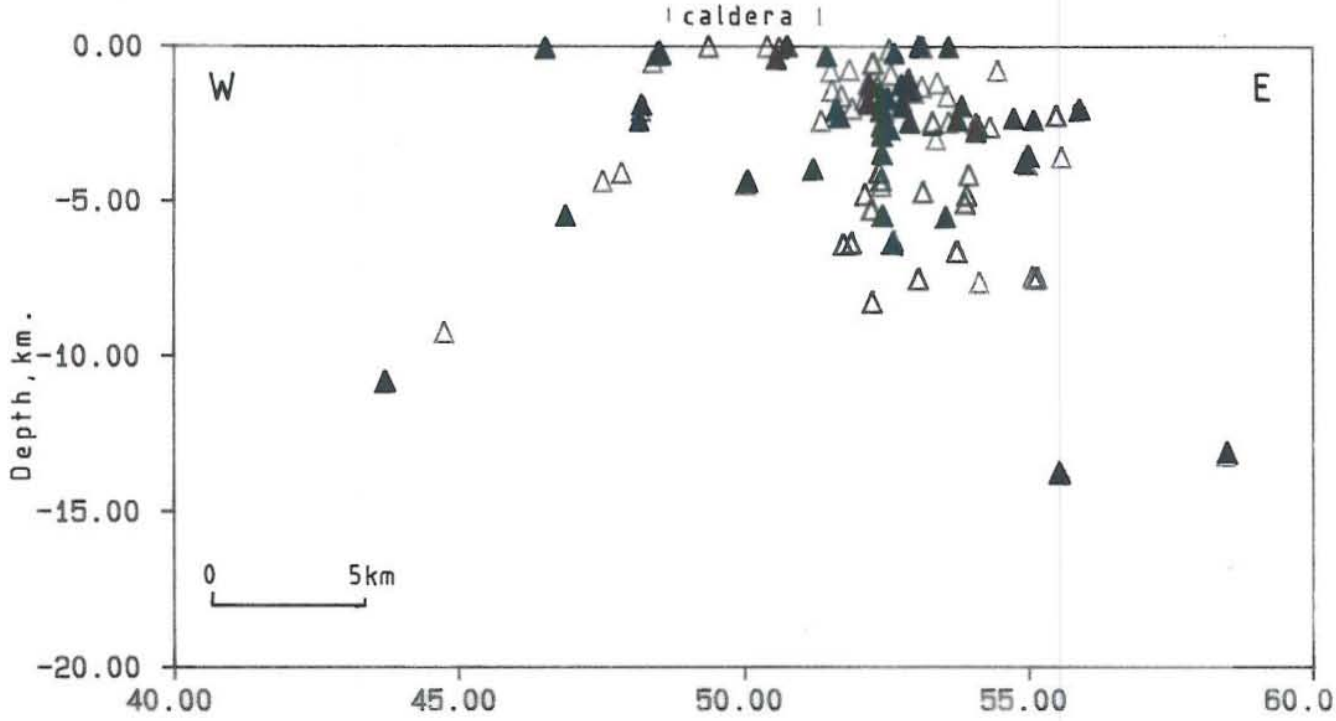

Figure 19. E-W section showing distribution of events at depths, along latitudes 1° 16.5' - 17.5', Lahendong geothermal area, Indonesia.

Legends :

▲ Events calculated from the first crustal velocity model.

Δ Events calculated from the second crustal velocity model.

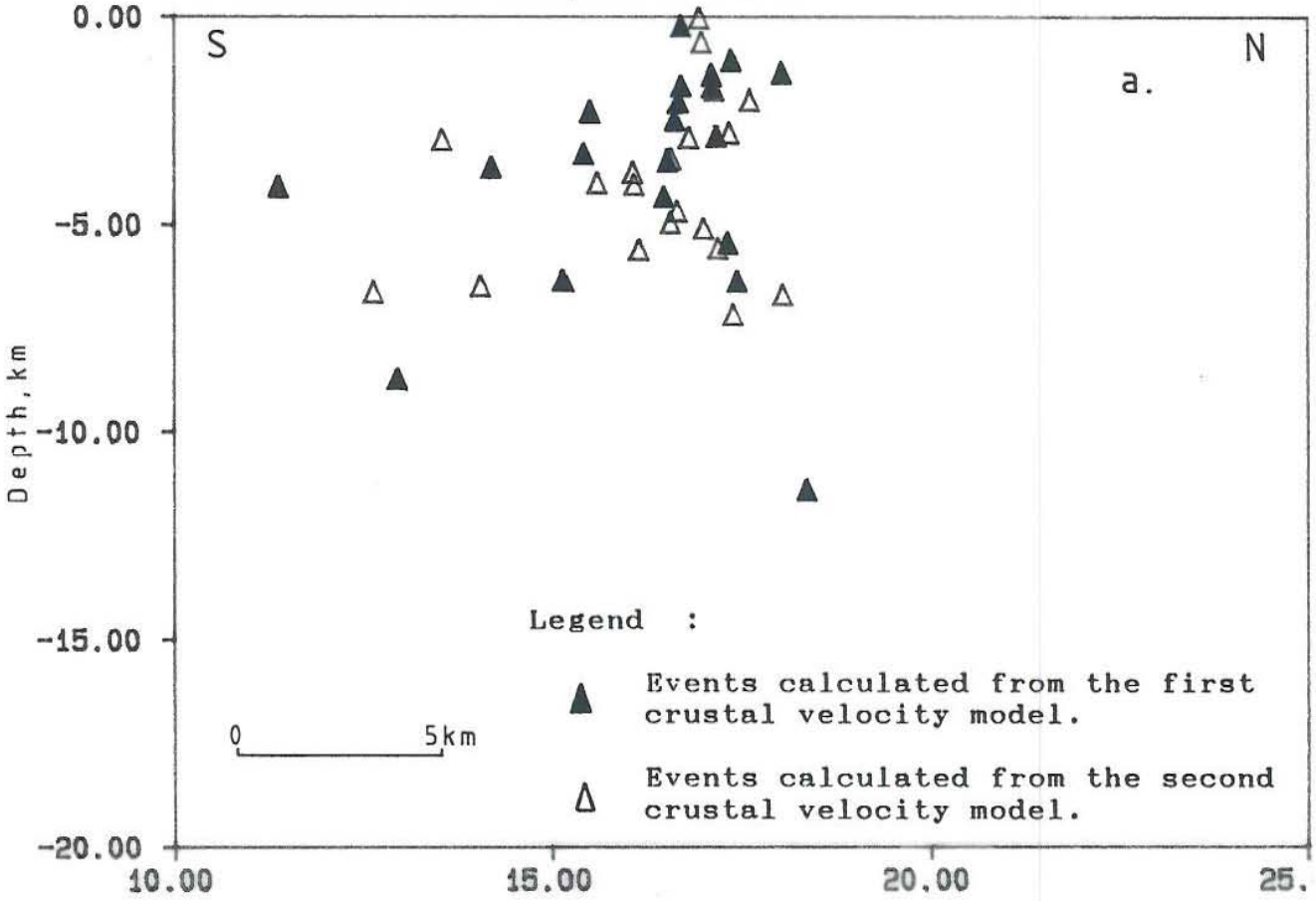

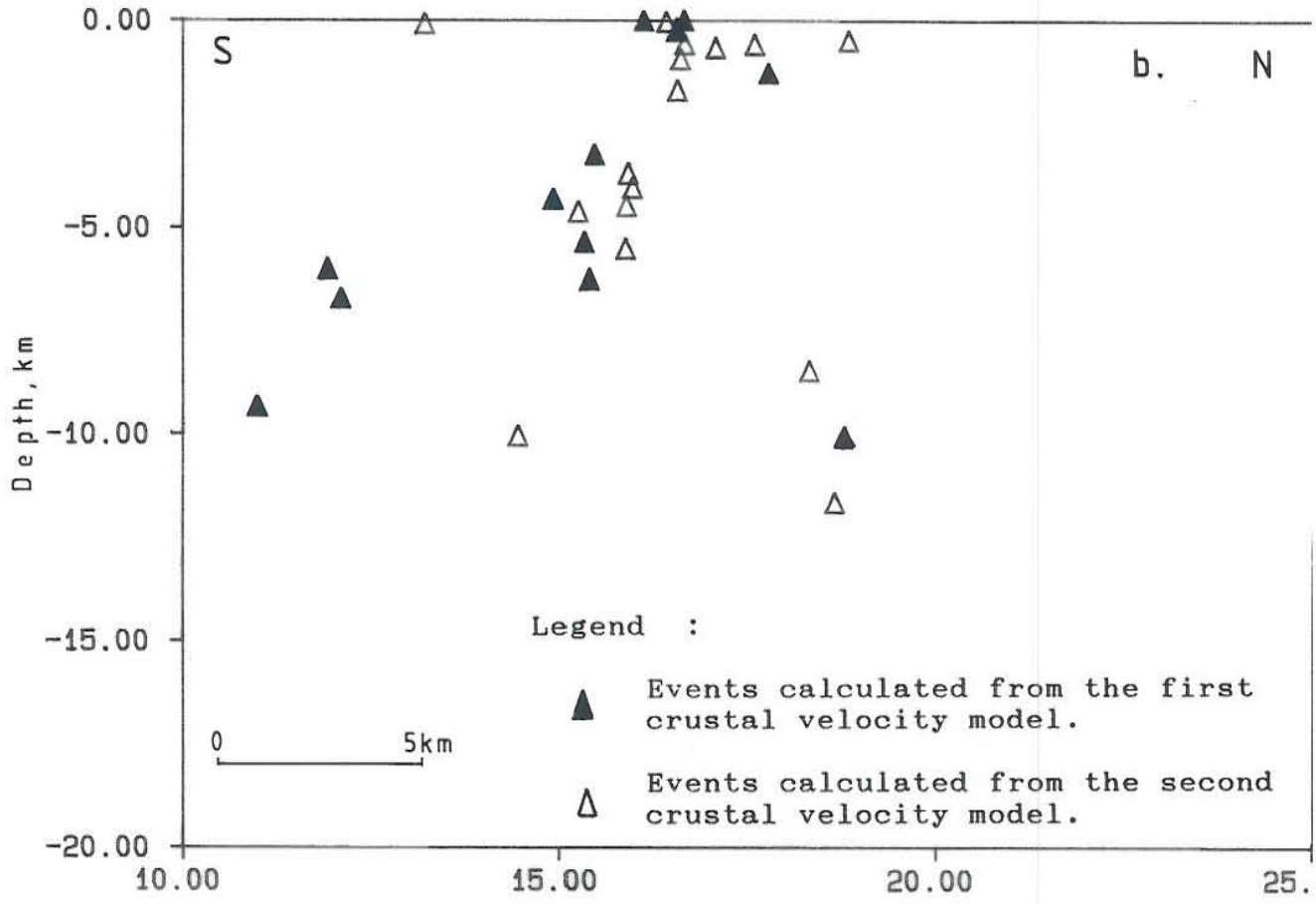

Figure 20. N-S sections showing distribution of events at depths, Lahendong geothermal area, Indonesia.
a. Along longitudes 124° 48.5′ - 49.5′ E,
b. Along longitudes 124° 52.5′ - 53.5′ E.

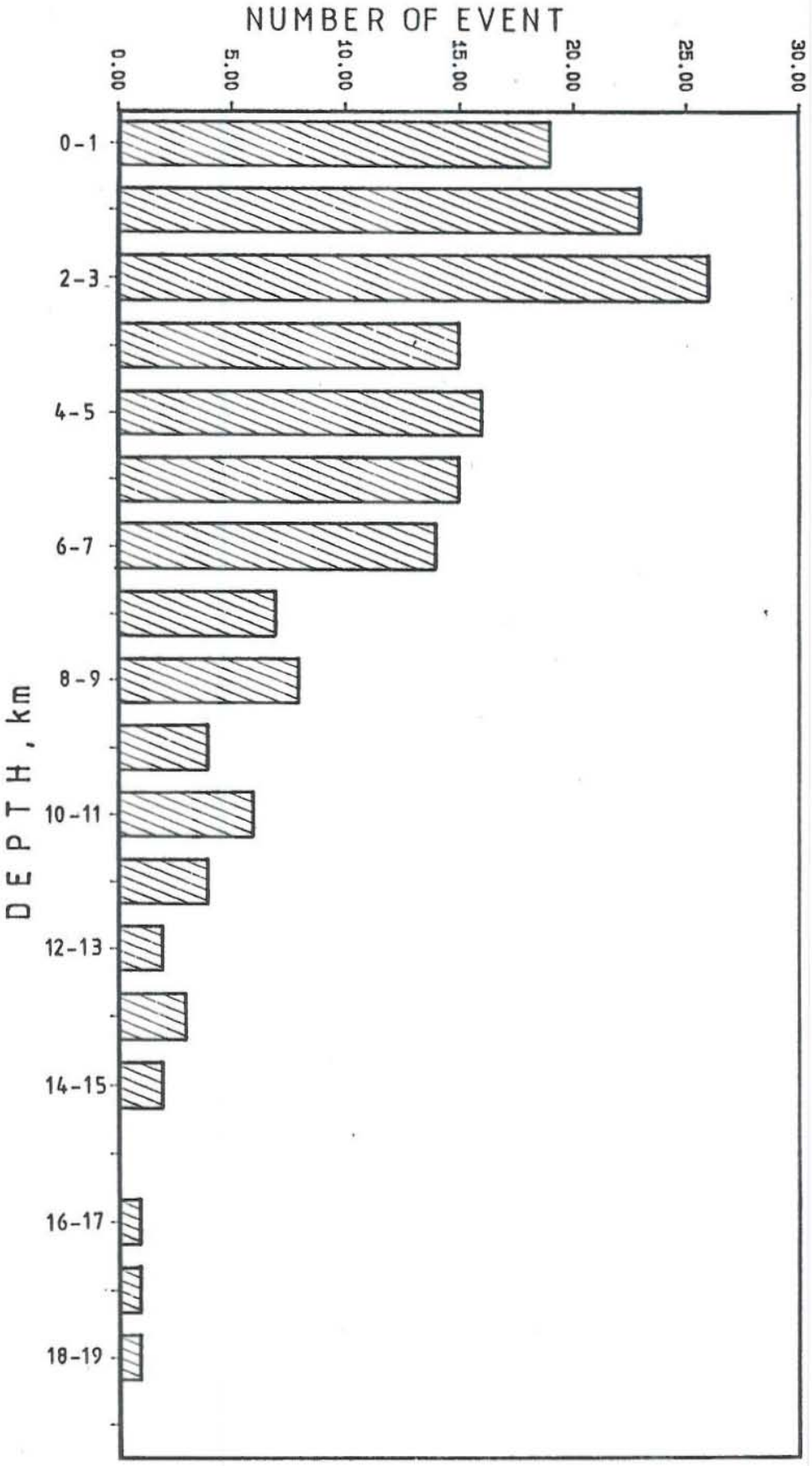

Figure 21. The diagram of number of events with depth showing a peak at shallow levels.